Environmental Health Perspectives
Vol. 73, pp. 53-75, 1987

Nonneoplastic Lesions of the Ovary in Fischer 344 Rats and B6C3F1 Mice

by Charles A. Montgomery* and Roger H. Alison*

The National Toxicology Program's pathology database on 2-year carcinogenicity studies was reviewed for nonneoplastic ovarian disease. Ovaries from 39,941 female Fischer rats and 41,444 female B6C3F1 mice were examined. A variety of inflammatory, degenerative, vascular, and proliferative lesions were documented and are described. The most common ovarian lesions in rats were cysts (6%). The most frequent ovarian lesions in mice were cysts (15%), acute inflammation (4%), degeneration (4%), vascular disease (2.5%), and atrophy (2%). There was no difference in incidence of ovarian disease between controls and treated animals. The frequency of ovarian disease in mice exceeded the frequency in rats in every category.

Introduction

The National Toxicology Program (NTP) has one of the largest pathology archives in the world, containing histopathology slides from more than 160,000 control and treated B6C3F1 mice and Fischer 344 rats. In toxicologic pathology, it is important that the pathologist know the morphology and incidence of spontaneous nonneoplastic disease in the rodent strain or target organ in question. Naturally occurring and toxic-induced ovarian disease in the B6C3F1 mouse and F344 rat is not well documented in the literature. NTP's unique rodent pathology database provided an opportunity to document and describe these characteristic lesions of the ovary.

Materials and Methods

The lesions reported in this paper were found during histological examination of control and treated animals from 2-year carcinogenicity studies conducted for the National Cancer Institute (NCI) and NTP. The majority of these studies contained control, low, and high dose groups, each of 50 male and 50 female rats and mice. The NTP data base at the time of this review contained 39,941 female Fischer 344 rats and 41,444 female B6C3F1 mice (Table 1). The animals were necropsied by or under the supervision of the laboratory pathologists. The ovaries were removed from the carcass, fixed in 10% buffered formalin, embedded in paraffin, sectioned at 5 to 6 μm, and stained with hematoxylin and eosin. Additional special stains were employed in some cases.

*National Toxicology Program, National Institute of Environmental Health Sciences, Research Triangle Park, NC 27709.

Table 1. Animals reviewed for nonneoplastic lesions of the ovary.

	Number of animals reviewed	
Treatment group	Rats	Mice
Treated	28,497	29,654
Control	11,444	11,490
Total	39,941	41,444

Table 2. Incidence of nonneoplastic lesions of the ovary.

	Incidence	
Lesion	Rats (%)	Mice (%)
Acute inflammation	0.5	4.0
Chronic inflammation	0.2	0.6
Degeneration	0.04	4.0
Pigments	0.03	0.3
Cysts	6.0	15.0
Vascular disease	0.1	2.5
Hyperplasia	0.1	0.5
Atrophy	0.2	2.0

Results and Discussion

The incidence of nonneoplastic lesions of the ovary in NTP B6C3F1 mice and F344 rats is shown in Table 2. There was no difference in incidence of ovarian disease between control and treated groups. The incidence of nonneoplastic ovarian lesions was greater in mice in every category examined.

Acute and Chronic Inflammation

Acute inflammatory lesions of the ovary included frank abscesses as well as focal or multifocal suppurative and necrotic changes within the ovarian parenchyma. There was an eightfold increase in incidence of lesions in mice over rats (Table 3). Nonneoplastic lesions of the

Table 3. Acute inflammation of the ovary.

	Number of cases			
	Rat		Mouse	
Type of inflammation	Treated	Control	Treated	Control
Abscess	71	17	498	238
Acute inflammation	113	17	740	346
Subtotal	184	34	1238	584
Total	218 (0.5%)[a]		1822 (4.0%)	

[a] Numbers in parentheses represent percent of total animals reviewed.

Table 4. Chronic inflammation of the ovary.

	Number of cases			
	Rat		Mouse	
Type of inflammation	Treated	Control	Treated	Control
Chronic inflammation[a]	36	18	153	74
Fat necrosis (steatitis)	10	4	4	4
Subtotal	46	22	157	78
Total	68 (0.2%)[b]		235 (0.6%)	

[a] Includes granulomatous/necrogranulomatous/chronic suppurative (active)/lymphocytic/plasmacytic inflammation and fibrosis/sclerosis.
[b] Numbers in parentheses represent percent of total animals reviewed.

ovary and uterus have been previously reported in NCI rats and mice (*1,2*).

In recent years, the NTP has recorded a significant increase in the number of B6C3F1 female mice with ovarian abscesses (Plate 1). The disease was observed in 2-year toxicity studies and generally did not occur in animals under 14 months of age. The ovarian abcesses were often large; many ruptured, resulting in peritonitis. An accompanying suppurative metritis was often observed (Plate 2). The incidence of ovarian abscesses ranged from less than 1% to 70% among 91 chronic studies, with an average incidence of 9%. There was a difference in the incidence of ovarian abscesses in mice from various breeding facilities, the rate ranging from 2.6 to 15.3%. Bacterial cultures from these abscesses were frequently positive for Klebsiella sp., particularly *Klebsiella oxytoca* (*3*). At NTP, the disease has been controlled by changing mouse vendor sources and implementing improved animal husbandry procedures at the testing laboratories.

The incidence of chronic inflammation of the ovary (Table 4) was lower than acute inflammation. Chronic inflammation consisted of cellular infiltration by lymphocytes, plasma cells, and macrophages (Plate 3), with or without fibrosis (Plate 4). Some lesions were characterized by granulomatous inflammation, with the ovarian parenchyma being replaced by foamy macrophages and multinucleated giant cells (Plate 5). Chronic inflammation of the ovary occasionally resulted in ovarian adhesions and/or inflammation of the oviduct or parovarian fat.

Degeneration

Degenerative lesions seen in mouse and rat ovaries consisted of dystrophic calcification or mineralization; osseous, squamous, and glandular metaplasia; hyalin, fatty, and mucoid degeneration; and amyloidosis (Table 5). The incidence of these lesions was 100 times greater in mice than in rats.

In addition, the mice examined had a 25-fold increased incidence of vascular disease compared to rats. Many of the degenerative lesions observed were secondary to vascular disease or older areas of hemorrhage, i.e., cholesterol clefts, dystrophic calcification (Plate 6), osseous metaplasia (Plate 7), and amyloidosis. Mineralization or concentrically laminated concretions (Psamomma bodies) in the ovary have also been described with fibrous tissue proliferation, neoplasia, and aging (*4–7*). Dystrophic calcification in multiple sites occurs in DBA/2, CBA, and NZB mouse strains (*8,9*). Focal areas of fatty change were occasionally observed in the rat ovary. These structures consisted of normal adipose tissue and did not compress the adjacent parenchyma (Plate 8). Similar lesions have been seen in the kidney, spleen, and liver of Fischer rats in NTP studies.

Amyloid deposition in the ovary was limited to the mouse in this series (Plate 9), but the incidence of amyloidosis was lower in the B6C3F1 mouse than previously reported in other mouse strains (*8,9*). Amyloidosis is particularly common in the luteinized tissue of DBA mice (*10*). In CD_1 mice, amyloid deposition may be so severe that it obscures the identity of the ovary (*9*).

An example of hyalin degeneration is shown in Plate 10. This change mainly affects the corpora lutea, which are gradually transformed into homogeneous, eosinophilic round masses in which secondary calcification may occur (*11*). Degenerative changes of the corpus luteum were seen in aged animals in this series (Plate 11).

Pigmentation

For the diagnoses coded as pigmentation (Table 6), the type of pigment was not specified. A re-examination of these ovaries revealed that in many instances, the pigment was yellow or yellow-brown, slightly granular, periodic-acid-Schiff positive, and acid-fast positive. This pigment, which was most often observed in atrophic ovaries, is compatible with ceroid (Plate 12). Ceroid in the ovary has been reported in 87.8% of female SD/Jcl rats (*12*). In C57BL mice, ceroid deposition may be ex-

Table 5. Degeneration of the ovary.

	Number of cases			
	Rat		Mouse	
Type of degeneration	Treated	Control	Treated	Control
Mineralization or calcification	4	2	90	33
Metaplasia[a]	0	0	3	3
Degeneration[b]	8	2	11	4
Amyloidosis	0	0	8	3
Subtotal	12	4	112	43
Total	16 (0.04%)[c]		155 (4.0%)	

[a] Osseous/squamous/glandular metaplasia.
[b] Hyalin/lipoid/mucoid degeneration.
[c] Numbers in parentheses represent percent of total animals reviewed.

Table 6. Ovarian pigments.

	Number of cases			
	Rat		Mouse	
Type of pigmentation	Treated	Control	Treated	Control
Pigmentation (unspecified)	3	3	30	47
Hemosiderin	4	0	8	5
Hematoidin	0	0	1	0
Melanin	0	0	0	1
Total	10 (0.03%)[a]		143 (0.3%)	

[a]Numbers in parentheses represent percent of total animals reviewed.

Table 7. Ovarian cysts.

	Number of cases			
	Rat		Mouse	
Type of cyst	Treated	Control	Treated	Control
Cyst[a]	1095	396	3125	1413
Follicular cyst	244	74	886	386
Corpus luteal cyst	27	23	7	7
Epidermoid cysts	0	0	3	0
Parovarian cyst	312	131	358	199
Subtotal	1678	624	4379	2005
Total	2302 (5.8%)[b]		6384 (15.4%)	

[a]Multiple/multilocular cyst, polycystic ovary, cystic degeneration and cystic hyperplasia.
[b]Numbers in parentheses represent percent of total animals reviewed.

tensive enough to impart a yellow color to the ovaries. This change has also been observed in ovarian tumors (*10*).

Hemosiderin and hematoidin pigment was observed occasionally and was usually associated with vascular lesions or old areas of hemorrhage (Plate 13). Two cases of melanin pigmentation of the ovary were seen in control mice (Plate 14). Melanin may be a component of ovarian teratomas in B6C3F1 mice (*13*).

Cysts

Ovarian cysts were a common finding in Fischer rats and B6C3F1 mice; mice had a threefold increased incidence of cysts over rats (Table 7). The overall incidence of 5.8% seen in Fischer rats was similar to that previously reported from this database (*2*). A comparison with other rodent strains is given in Table 8.

Follicular cysts arise in secondary follicles that fail to ovulate or that become atretic. These cysts vary in size and may be single or multiple (Plates 15 and 16). Cysts frequently secrete estrogen in excessive amounts, resulting in persistent estrus, cystic endometrial hyperplasia, and infertility (*14*). Cystic endometrial hyperplasia of the uterus is extremely common in B6C3F1 mice, with an incidence greater than 35% (*15*). If young female rats or mice are subjected to room light for 24 hr/day instead of alternating cycles of light and darkness, their estrous cycles will stop between 1 and 3 months, and constant estrus will supervene. The ovaries from such animals have few or no corpora lutea, atypical cystic follicles, and abundant stroma. Hypophysectomized animals do not show these responses to constant light (*16*). Similar results can be demonstrated with a single injection of 5 to 100 mg of testosterone proprionate given on the fifth day of life (*17,18*). Follicular cysts induced by constant illumination are reversible when light cycle is returned to normal. The estrous cycles reappear and the ovaries become normal in gross and microscopic appearance (*19*). In older, irregularly cycling rats, preovulatory follicles develop but many do not ovulate. These nonovulatory follicles form ovarian cysts that remain within the ovary. The number of cysts increases with age, forming a polycystic ovary (Plate 17); these animals then enter a state of constant estrus (*20*). Histologically, follicular cysts may be distinguished from normal Graafian follicles by the absence of an oocyte, the profusion of follicular fluid, and characteristically, by the thin wall of the cyst (Plate 18). Larger follicular cysts often possess a thin fibrous outer layer lined on the inner surface by one or two layers of cuboidal or flattened granulosa cells (Plate 19) (*14*).

Table 8. Incidence of ovarian cysts by strain.

Species	Strain	Rate of occurrence, %	Reference
Rats	Osborne-Mendel	3.2	(*43*)
	Fischer	6.6	(*2*)
	WAG/Rij	54.0	(*32*)
	BN/Bi	3.0	(*32*)
	WAG/Rij X BN/Bi F_1	19.0	(*32*)
Mice	B6C3F_1	11.0	(*15*)
	CBA	80.0	(*44*)
	BALB/c, virgin	17.1	(*30*)
	BALB/c, breeder	8.1	(*30*)
	CVA	50.0	(*8*)
	RFM	30.0	(*8*)
	C57/BL	34.0	(*8*)
	NZB	2.0	(*8*)

Lutein cysts or cystic corpora lutea may serve as a source of prolonged, noncyclic progesteronic stimulation. Microscopically, a lutein cyst has a large, fluid-filled central cavity. Its wall consists of several layers of granulosa-luteal cells. These cells are large polyhedral cells with abundant, foamy, eosinophilic cytoplasm that contains variable numbers of fat droplets (Plate 20) (*14*).

Parovarian cysts are vesicular structures located in the mesovarium or mesosalpinx and are thought to arise from vestigial remnants of the rostral ends of the mesonephric and paramesonephric ducts. These cysts are lined by cuboidal epithelium and are surrounded by smooth muscle (Plate 21). Parovarian cysts must be distinguished from cystic distention of the rete tubules, which lack smooth muscle in their cyst wall (Plate 22) (*21*). DBA mice frequently have degrees of cystic degeneration from dilatation of the rete tubules. These cysts often deform the entire ovary. Cystic degeneration should be differentiated from cystic enlargement of the bursa, which is frequently found in old mice (Plate 15). An enlarged bursa collapses at dissection, disclosing the ovary lying within. True ovarian cysts can be dis-

sected intact, and ovarian tissue is found in their walls (*11*).

Epidermoid cysts in this series were all diagnosed in B6C3F1 mice. Ovarian epidermoid cysts were lined by squamous epithelium and produced keratin (Plate 23). Several malignant tumors have been reported to arise from ovarian dermoid cysts (benign cystic teratoma) in women (*22*). More than 80% of these tumors are squamous cell carcinomas. There is one reported case in the literature of a Wistar rat that had a squamous cell carcinoma of the ovary that arose from an epidermoid cyst. The animal had been treated with 7,12-dimethylbenz[a]anthracene (*23*). Other cysts also occur, the origin of which has been variously attributed to rete tubules or misplaced embryonic structures. Such cysts are lined by epithelium, which may be ciliated or which is high columnar with acidophilic cytoplasmic droplets that are periodic-acid-Schiff positive. These cysts show a tendency toward papilliferous growth (Plates 24 and 25). They may occur early in life but are more common and larger later in life (*10*).

Vascular lesions

Vascular lesions and their sequelae were primarily limited to the mouse, where there was a 25-fold increase in disease incidence over rats (Table 9). An occasional diagnosis of hemorrhage or thrombosis was made in the Fischer rat, but surprisingly, no diagnosis of periarteritis-nodosa (PAN) was made in the ovarian artery or associated branches. PAN has recently been reviewed by Anver and Cohen (*24*); differences in incidence between rat strains were given, but data on Fischer rats were not available. In NTP studies, the overall incidence of PAN has been comparatively low. Seven cases of periarteritis were present in mice in this series. The diagnoses of arteriosclerosis and perivasculitis were made in two of these cases. The lesions were in the ovarian artery or its branches and consisted of periadventitial fibrosis, medial hypertrophy, medial fibrinoid necrosis, and endothelial hypertrophy or hyperplasia (Plate 26). Similar lesions have been reported in O_{20}, C57BL, NZB/BL, RF, RFM, PN, and BL/De strains of mice (*11,8,25,26*).

In the B6C3F1 mouse, hemorrhagic cysts (Plate 27), acute and chronic hemorrhage with thrombosis (Plate 28), and angiectasis were commonly seen within the ovary. Old areas of hemorrhage often contained hemosiderin-laden macrophages, hematoidin pigment, cholesterol clefts, dystrophic calcification, amyloid deposition, or fibrosis. Diagnoses of hemorrhagic cysts were not made for the normally occurring corpus hemorrhagicum of the mouse ovary. Angiectasis consisting of dilated channels lined by large, plump, often pleomorphic endothelium was a frequent finding (Plate 29). These vascular lesions, most often seen in aged mice, had to be differentiated from hemangiomas and hemangiosarcomas of the ovary. This diagnostic difficulty has been noted by others (*10,5,27*).

Of related interest was the unusually high percentage of vascular ovarian tumors documented in this same database (*13*). Why the mouse is more prone to vascular disease is unknown. Hemorrhage and thrombosis with secondary mineralization and cholesterol clefts were seen in these B6C3F1 mice and have been reported in other mouse strains with granulosa cell tumors (*6,28*). Ovarian angectasia has been reported in other mouse strains unrelated to neoplasia (*5,10,29*). The lesion is more common in virgin females than in breeders. Frith (*30*) has reported ovarian hemorrhage and angiectasis in 4.4% of BALB/c mice between 319 and 500 days of age. Breeder females showed a zero incidence for the same time frame. Telangiectasis principally affecting vessels in the ovary, uterus, and small intestine (83.3%) was a common finding in NZC/BL mice treated with 7,12-dimethylbenz[a]anthracene (*31*).

Table 9. Vascular lesions of the ovary.

	Number of cases			
	Rat		Mouse	
Type of lesion	Treated	Control	Treated	Control
Hemorrhagic cyst	3	3	425	286
Hemorrhage	10	1	100	35
Hematoma	2	0	41	17
Thrombosis	1	0	35	15
Angiectasia	0	0	58	17
Periarteritis	0	0	3	4
Subtotal	16	4	662	374
Total	20 (0.05%)[a]		1036 (2.5%)	

[a]Numbers in parentheses represent percent of total animals of that species reviewed.

Table 10. Hyperplasia of the ovary.

	Number of cases			
	Rat		Mouse	
Type of hyperplasia	Treated	Control	Treated	Control
Epithelial hyperplasia[a]	6	3	147	24
Other[b]	18	9	31	7
Subtotal	24	12	178	31
Total	36 (0.1%)[c]		209 (0.5%)	

[a]Adenomatous/tubular/papillary hyperplasia.
[b]Granulosa cell/interstitial (stromal) cell hyperplasia.
[c]Numbers in parentheses represent percent of total animals of that species reviewed.

Table 11. Atrophy of the ovary.

	Number with atrophy of ovary			
	Rat		Mouse	
	Treated	Control	Treated	Control
	56	42	597	241
Total	98 (0.2%)[a]		838 (2.0%)	

[a]Numbers represent percent of total animals of that species reviewed.

Hyperplasia

This diagnosis was reported in less than 1% of the rats and mice in this series (Table 10). In rats, the morphological qualifiers of adenomatous, tubular, or

papillary were used for epithelial hyperplasia to describe an increase in Sertoli-like tubules or cords in atrophic ovaries (Plate 30). These structures have been described by others (*7,32–35*) and were characterized by focal areas of epithelial cells with vague cytoplasmic borders and nuclear characteristics similar to those of the Sertoli cells of the seminiferous tubule. These tubules contained a distinct basement membrane but lacked other spermatogenic elements. They were most often located near the hilus of the ovary. The formation of testislike tubules similar to those seen in senile ovaries can be observed in rats hypophysectomized at 26 days of age (*34*). The tubules occur as early as 5 months of age but are most common at 11 months. The formation of these structures is thought to be associated with a deficiency in gonadotropins (*34*). Tubular hyperplasia of the ovary has been described in the Sprague-Dawley rat (*36*). It may be differentiated from adenoma by size and the absence of compression.

Epithelial hyperplasia was much more common in B6C3F1 mice. Downgrowth of the overlying ovarian epithelium was so extensive in some cases that the ovary was replaced by interlacing clefts and tubules lined by cuboidal to columnar epithelium resembling the germinal epithelium (Plate 31). Tubular downgrowths are infrequent in most mouse strains, but are common in CBA mice (*10*). Irradiation increases tubular proliferation in aged mice (*10*). Distinction between tubular hyperplasia and adenoma is difficult (*10,37*). Adenomas are composed of a distinct mass of tubulo-stromal elements, may compress adjacent tissues, and are usually 2 to 3 mm or more in diameter (*38*). Interstitial cell hyperplasia (Plate 32) and hypertrophy are commonly seen in ovaries with follicular atrophy. Hypertrophy of interstitial cells can occur as a host response to toxic injury in the absence of ovarian atrophy. In the NTP subchronic study of tricresyl phosphate, this type of lesion was observed (Plate 33). Granulosa cell hyperplasia has occasionally been observed (Plate 34) (*32*).

Atrophy

Ovarian atrophy occurred in mice 10 times more often than in rats (Table 11) and was associated with aging (Plate 35). Morphologically, there is a diminution in size and weight of ovaries in older mice. Microscopically, there is a decrease in the number of follicles and/or increase in the number of cystic follicles. Corpora lutea are decreased in number; in mice, corpora lutea show a tendency toward hyalinization and amyloid deposition. There is a marked increase in interstitial cells, many of which contain ceroid pigment (*7,11,33*). Nude mice, neonatally thymectomized mice, or rats and rodents treated with hormones or irradiation have ovarian dysgenesis or atrophy (*32,33,39–41*). Ovarian atrophy resulting from urethane injection in neonatal mice has been described in C57/BL6J mice (*42*). In the NTP subchronic toxicity study of vinylcyclohexene, a marked dose-related follicular atrophy in the mouse was observed (Plate 36).

REFERENCES

1. Ward, J. M., Goodman, D. G., Squire, R. A., Chu, K. C., and Linhart, M. S. Neoplastic and nonneoplastic lesions in aging (C57B1/6N × C3H/HeN)F1 (B6C3F1) mice. JNCI 63: 849–854 (1979).
2. Goodman, D. G., Ward, J. M., Squire, R. A., Chu, K. C., and Linhart, M. S. Neoplastic and nonneoplastic lesions in aging in F344 rats. Toxicol. Appl. Pharmacol. 48: 237–248 (1979).
3. Rao, G. N., Hickman, R. L., Seilkop, S. K., and Boorman, G. A. Utero-ovarian infection in aged B6C3F1 mice. Lab. Anim. Sci. 37 (2), in press.
4. Sally, R. E. Tumors of the ovary and maldeveloped gonads. Atlas of Tumor Pathology. Second series, Fascicle 166, Armed Forces Institute of Pathology, Washington, DC, 1979.
5. Frith, C. H., Zuna, R. E., and Morgan, K. A morphological classification and incidence of spontaneous ovarian neoplasms in three strains of mice. JNCI 67: 693–702 (1981).
6. Rehm, S., Dierksen, D., and Deerberg, F. Spontaneous ovarian tumors in Han:NMRI Mice: histologic classification, incidence, and influence of food restriction. JNCI 72: 1383–1395 (1984).
7. Russfield, A. B. Pathology of the endocrine glands, ovary, and testis of rats and mice. In: Pathology of Rats and Mice (E. Cotchin and F. J. C. Rowe, Eds.), Blackwell Scientific Publications, Oxford, England, 1967, pp. 391–467.
8. Zurcher, C., vanZwieten, M. J., Solleveld, H. A., and Hollander, C. F. Aging research. In: The Mouse in Biomedical Research. Vol. 4, Experimental Biology and Oncology (H. L. Foster, J. D. Small, and J. G. Fox, Eds.), Academic Press, New York, 1982, pp. 11–35.
9. Burek, J. D., Molello, J. A., and Warner, S. D. Selected nonneoplastic diseases. In: The Mouse in Biomedical Research. Vol. 3, Diseases (H. L. Foster, J. D. Small, and J. G. Fox, Eds.), Academic Press, New York, 1982, pp. 425–440.
10. Lemon, P. G., and Gubareva, A. V. Tumors of the ovary. In: Pathology of Tumors in Laboratory Animals. Tumors of the Mouse (V. S. Turusov, Ed.), IARC Scientific Publications, Lyon, 1979, pp. 385–410.
11. Thung, P. L., Boot, L. M., and Mulhbock, O. Senile changes in the oestrous and in ovarian structure in some inbred strains of mice. Acta Endocrinol. 23: 8–32 (1956).
12. Muraoka, Y., Itoh, M., Maeda, Y., and Hayashi, Y. Histological changes of various organs in aged SD-JCL rats. Exp. Animal. 26: 1–12 (1977).
13. Alison, R. H., Morgan, K. T., Haseman, J. K., and Boorman, G. A. Morphology and classification of ovarian neoplasms in F344 rats and B6C3F1 mice. JNCI 78(6): 293–307 (1987).
14. King, N. W. The reproductive tract. In: Pathology of Laboratory Animals. Vol. 1 (K. Benirschke, F. M. Garner, and T. C. Jones, Eds.), Springer-Verlag, New York, 1978, pp. 509–580.
15. Goodman, D. G., Boorman, G. A., and Strandberg, J. D. Selection and use of the B6C3F1 mouse and F344 rat in long-term bioassay for carcinogenicity. In: Handbook of Carcinogen Testing (H. A. Milman and E. K. Weisburger, Eds.), Noyes Publications, Park Ridge, NJ, 1985, pp. 282–320.
16. Murthy, A. S. K., and Russfield, A. B. Endocrine changes in two strains of mice exposed to constant illumination. Endocrinology 86: 914–917 (1970).
17. Russfield, A. B. Experimental endocrinopathies. Meth. Achiev. Exp. Pathol. 7: 132–148 (1975).
18. Sawada, T., and Kosaka, T. Morphological recovery in the polycystic ovaries of persistent-estrus rats induced by continuous illumination. Jikken Dobutsu 30: 487–490 (1981).
19. Singh, K. Induction of polycystic ovarian disease in rats by continuous light. I. The reproductive cycle, organ weights and histology of the ovaries. Am. J. Obstet. Gynecol. 103: 1078–83 (1969).
20. Peluso, J. J., Steger, R. W., Huang, H., and Meites, J. Pattern of follicular growth and steroidogenesis in the ovary of aging cyclic rats. Exp. Aging Res. 5: 319–333 (1979).
21. Nielsen, S. W., Misdorp, W., and McEntee, K. XV tumors of the ovary. Bull. WHO 53: 203–215 (1976).
22. Scully, R. E. Ovarian tumors. Am. J. Pathol. 87: 686–720 (1977).
23. Nishida, T., Oda, T., Sugiyama, T., Nishida, T., Nishimura, H.,

Tsunawaki, A., and Yakushiji, M. Squamous cell carcinoma arising from an epidemoid cyst in the ovary of a rat treated with 7,12-dimethylbenz[a]anthracene. Gann 73: 153–157 (1982).
24. Anver, M. R., and Cohen, B. J. Lesions associated with aging. In: The Laboratory Rat. Vol. 2, Biology and Disease (H. J. Baker, J. R. Lindsay, and S. H. Weisbroth, Eds.), Academic Press, New York, 1979.
25. Upton, A. C., Conklin, J. W., Cosgrove, G. E., Gude, W. D., and Darden, E. B. Necrotizing polyarteritis in aging RF mice. Lab. Invest. 16: 483–487.
26. Wigley, R. D., and Couchman, K. G. Polyarteritis nodosa-like disease in outbread mice. Nature 211: 319–320 (1966).
27. Goodman, D. G., and Strandberg, J. D. Neoplasms of the female reproductive system. In: The Mouse in Biomedical Research. Vol. 4, Experimental Biology and Oncology (H. L. Foster, J. D. Small, and J. G. Fox, Eds.), Academic Press, New York, 1982, pp. 397–411.
28. Carter, R. L. Pathology of ovarian neoplasms in rats and mice. Eur. J. Cancer 3: 537–543 (1968).
29. Slye, M., Holmes, H. F., and Wells, H. G. Primary spontaneous tumors of the ovary in mice. Studies on the incidence and inheritability of spontaneous tumors in mice. J. Cancer Res. 5: 205–226 (1920).
30. Frith, C. H., Highman, B., Burger, G., and Sheldon, W. D. Spontaneous lesions in virgin and retired breeder BALB/c and C57BL/6 mice. Lab. Anim. Sci. 33: 273–286 (1983).
31. Geary, C. P. Carcinogen-induced granulosa cell tumors in the NZB/BL mice. Pathology 16: 131–135 (1984).
32. Burek, J. D. Pathology of Aging Rats. CRC Press Inc., West Palm Beach, FL, 1978, pp. 117–123.
33. Labhsetwar, A. P. Ageing changes in pituitary-ovary relationships. J. Reprod. Fert. Suppl. 12: 99–117.
34. Arias, M., and Aschheim, P. Hypophysectomy and aging. Primary or secondary ovarian senescence. Experientia 30: 213 (1974).
35. Engle, E. T. Tubular adenomas and testis-like tubules of the ovaries of aged rats. Cancer Res. 6: 578–582 (1946).
36. Gregson, R. L., Lewis, D. J., and Abbott, D. P. Spontaneous ovarian neoplasms of the laboratory rat. Vet. Pathol. 21: 292–299 (1984).
37. Murphy, E. D. Hyperplastic and early neoplastic changes in the ovaries of mice after genic deletion of germ cells. JNCI 48: 1283–1295 (1972).
38. Morgan, K. T., and Alison, R. H. Tubular adenoma, ovary, mouse. In: Pathology of Laboratory Animals. Vol. 5, Genital System (T. C. Jones, Ed.), Springer-Verlag, New York, 1986.
39. Michael, S. D., Taguchi, O., and Nishizuka, Y. Effect of neonatal thymectomy on ovarian development and plasma LH, FSH, GH, and PRL in the mouse. Biol. Reprod. 22: 343–350 (1980).
40. Jones, L. A., and Bern, H. A. Long-term effects of neonatal treatment with progesterone, alone and in combination with estrogen, on the mammary gland and reproductive tract of female BALB/cfC3H mice. Cancer Res. 37: 67–75 (1977).
41. Lintern-Moore, S. Effect of athymia on the initiation of follicular growth in the rat ovary. Biol. Reprod. 17: 150–161 (1977).
42. Davis, N. E. T. Ovarian atrophy resulting from urethane injection of neonatal mice. J. Reprod. Fert. 51: 159–161 (1977).
43. Goodman, D. G., Ward, J. M., Squire, R. A., Paxton, M. B., Reichardt, W. D., Chu, K. C., and Linhart, M. S. Neoplastic and nonneoplastic lesions in aging Osborne-Mendel rats. Toxicol. Appl. Pharmacol. 55: 433–447 (1980).
44. Gosden, R. G., Jones, E. C., and Jacks, F. Pituitary-ovarian relationships during the post-reproductive phase of inbred mice. Exp. Gerontol. 13: 159–166 (1978).

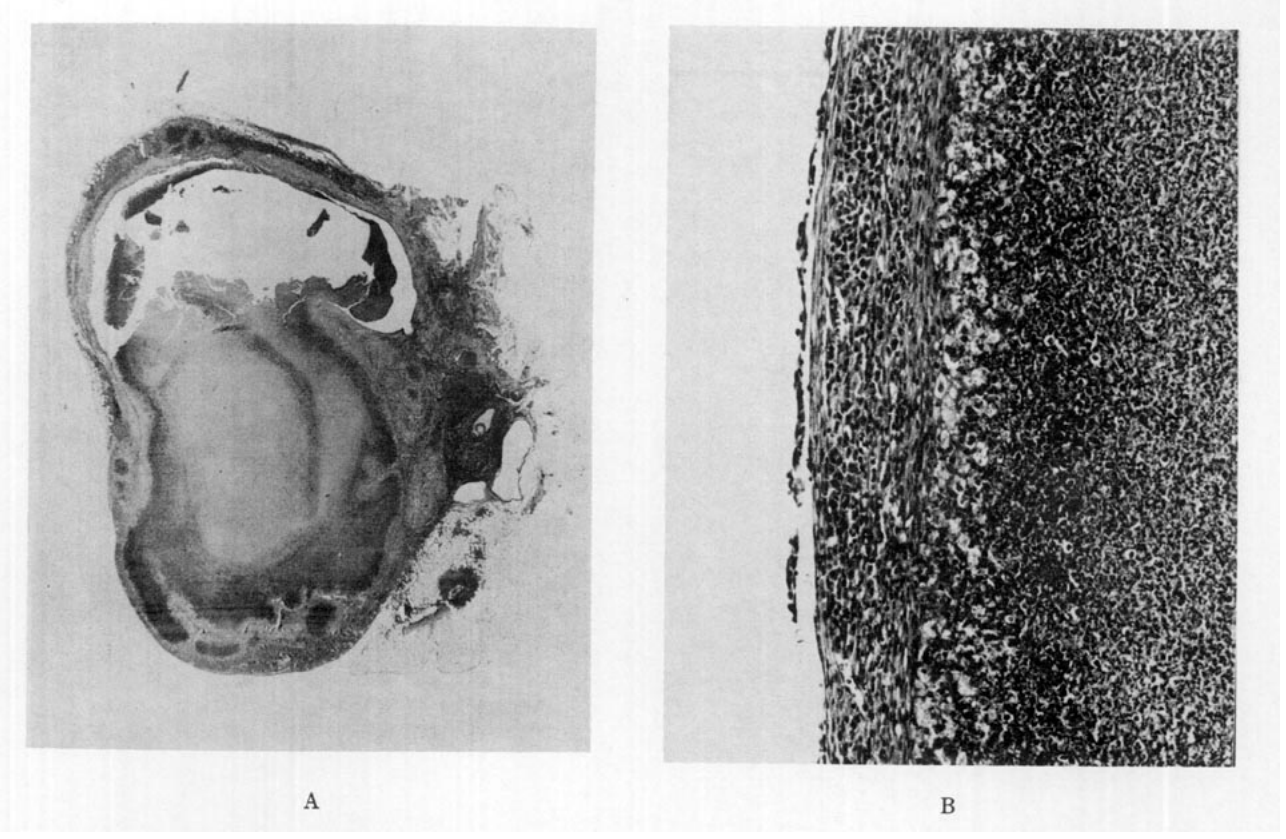

PLATE 1. Low power photomicrograph of an ovarian abscess in a B6C3F1 mouse. (*A*) The necrosuppurative process has replaced the majority of the ovarian parenchyma. (*B*) Wall of abscess (left) with zone of necrosis and polymorphonuclear leukocytes (right).

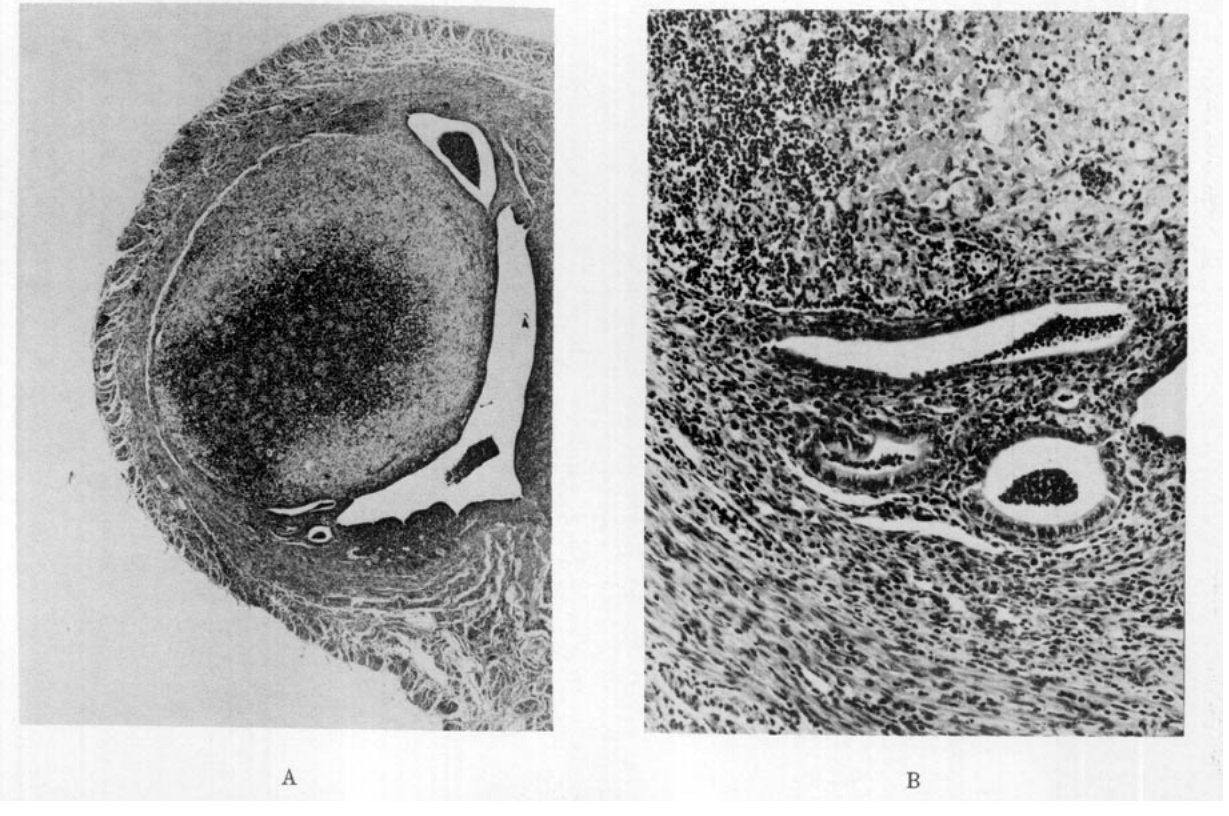

PLATE 2. Suppurative metritis in a B6C3F1 mouse. (*A*) Low power photomicrograph shows large abscess in wall of uterus with impingement on the lumen. (*B*) Higher magnification demonstrates dilated endometrial glands filled with polymorphonuclear leukocytes.

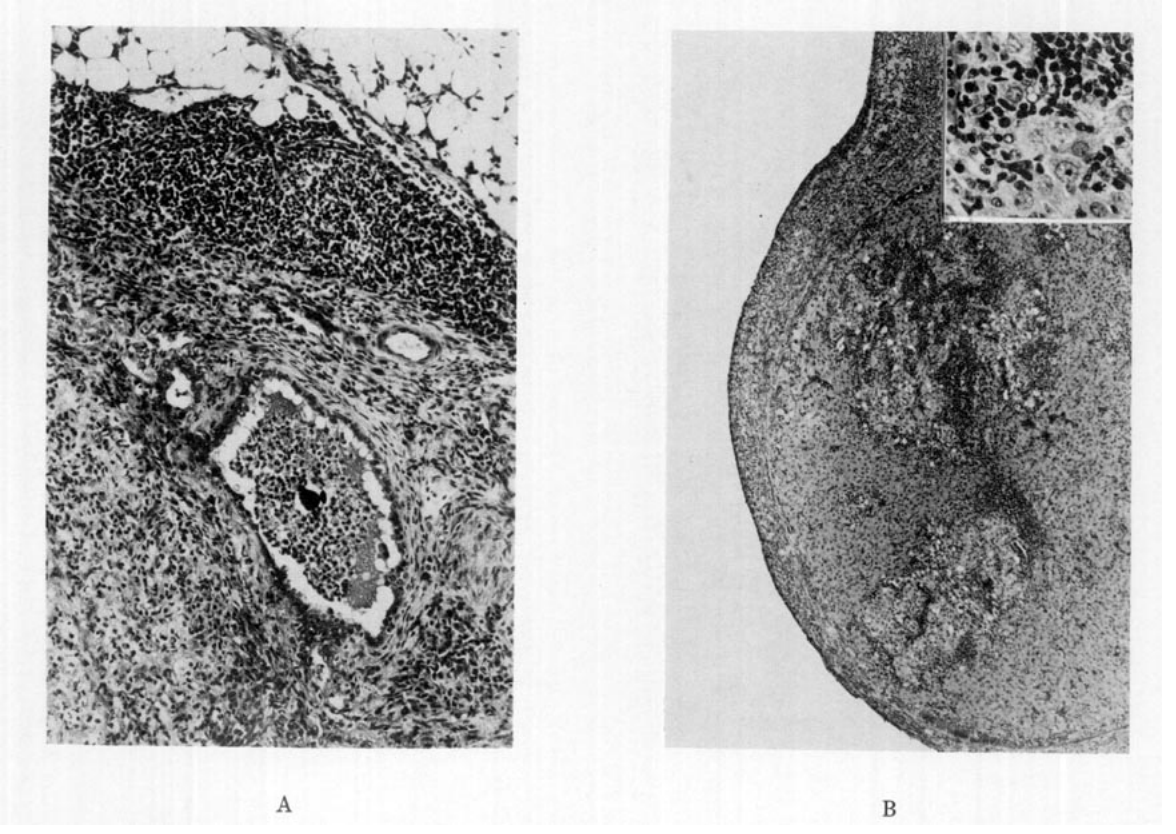

PLATE 3. Chronic inflammation of the ovary in a F344 rat. (*A*) Infiltration of lymphocytes and plasma cells in ovarian capsule, parovarian fat, and perifollicular interstitial tissue. (*B*) Chronic inflammation of the corpus leuteum. Inset: lymphocytes and macrophages adjacent to luteal cells.

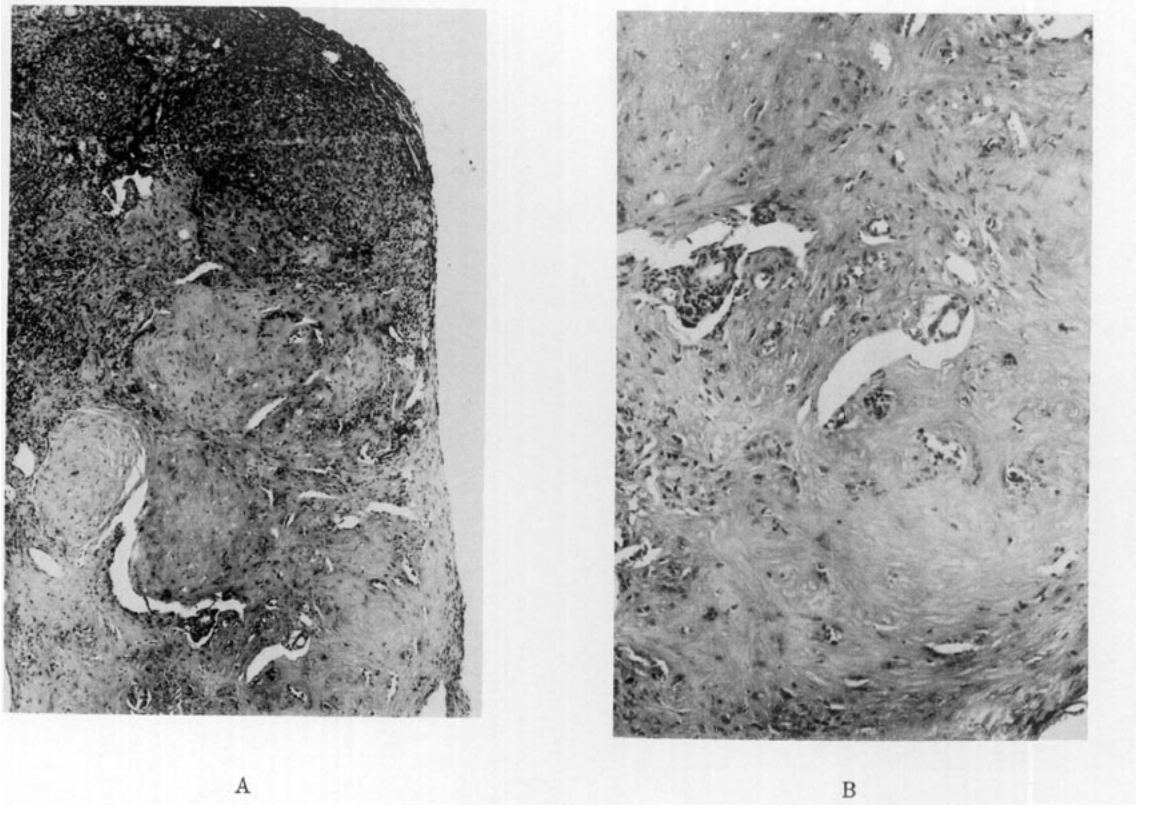

PLATE 4. Fibrosis of the ovary in a B6C3F1 mouse. (*A*) Fibrous connective tissue has replaced half the ovary. (*B*) Dense collagen is anisotropic under partially polarized light.

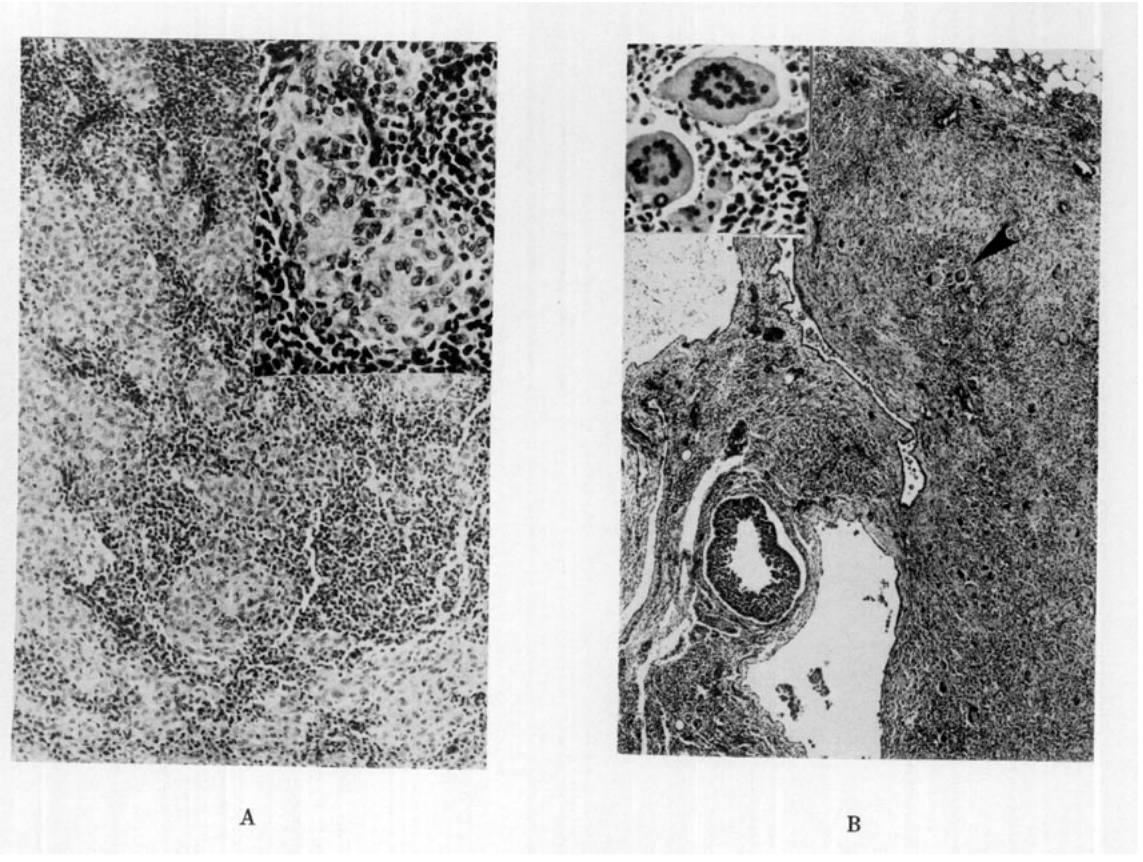

PLATE 5. (*A*) Granulomatous oophoritis in a F344 rat. Inset: Multifocal aggregates of foamy macrophages surrounded by lymphocytes. (*B*) Diffuse granulomatous inflammation of the ovary in a F344 rat with giant cells (→). Inset: multinucleated giant cells.

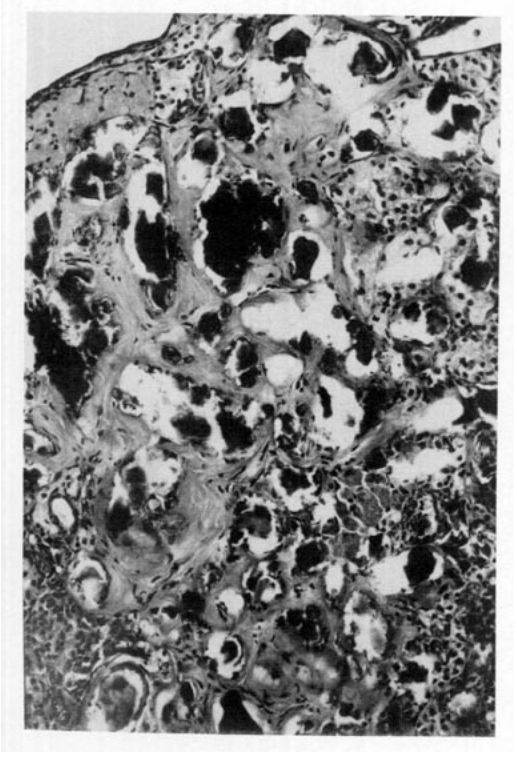

PLATE 6. Photomicrograph of dystrophic calcification in the ovary of a B6C3F1 mouse.

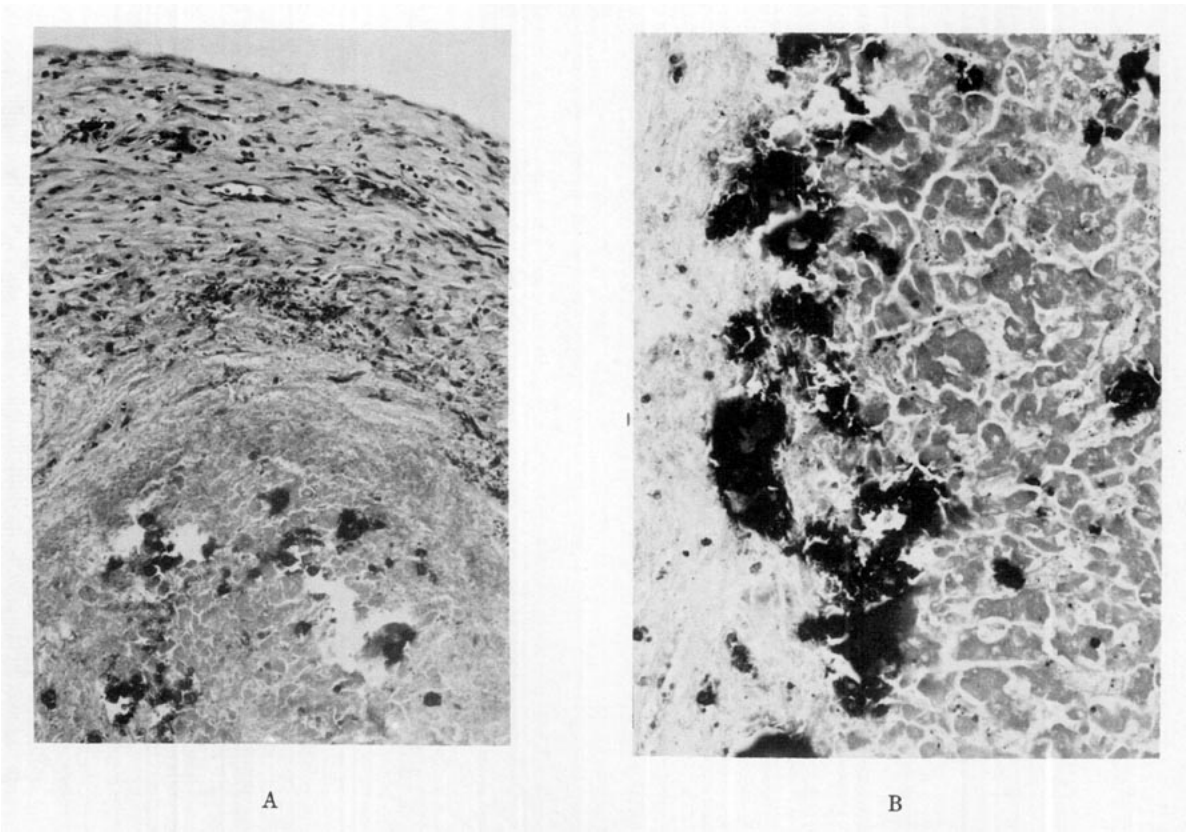

PLATE 7. Osseous metaplasia of the ovary in area of old hemorrhage in a B6C3F1 mouse. (*A*) Ovarian capsule is thickened by fibrous connective tissue (top). Osseous metaplasia is seen below. (*B*) Higher magnification showing dystrophic calcification (left) and osteoid (right).

PLATE 8. Focal area of fatty change in ovarian parenchyma of a F344 rat.

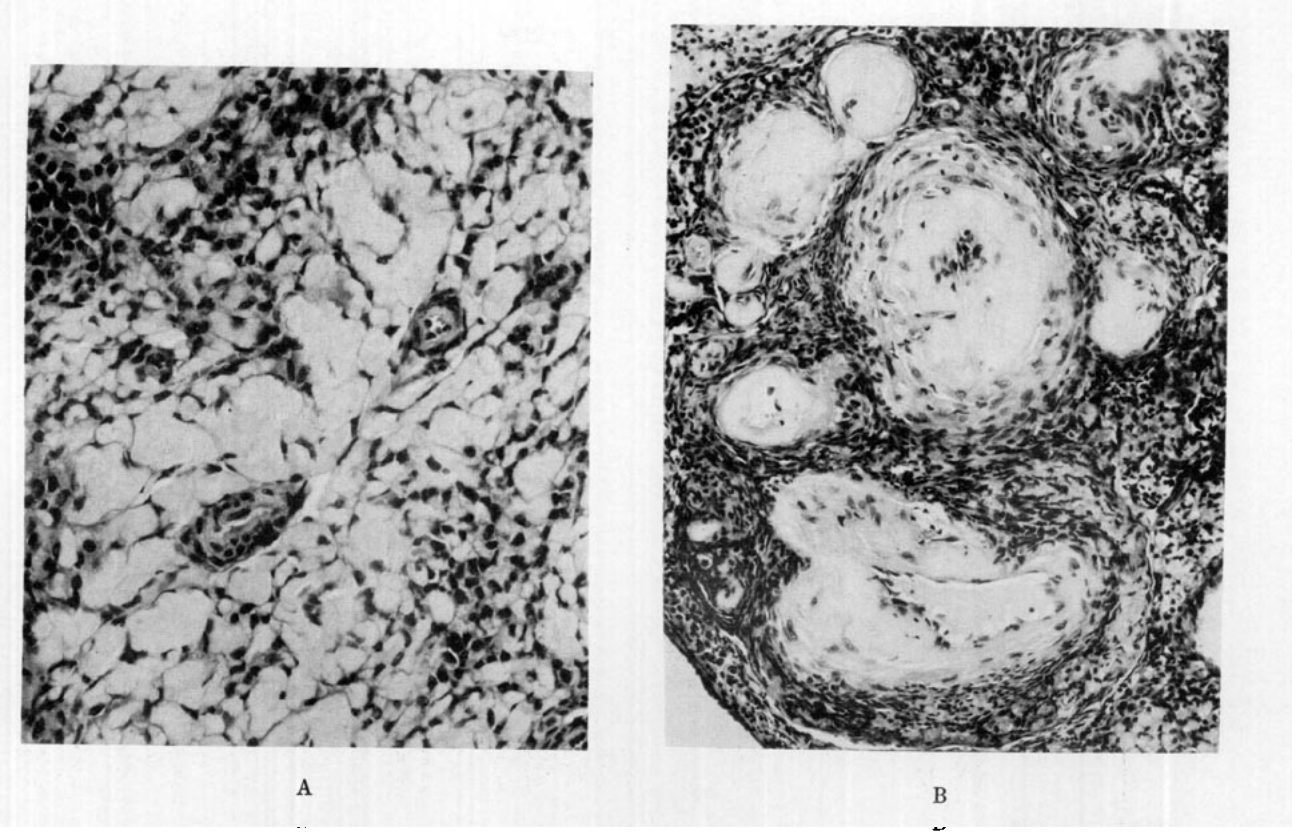

PLATE 9. Three types of ovarian amyloidosis observed in B6C3F1 mice. (*A*) Intracellular amyloid deposition within parenchyma. (*B*) Amyloid deposition in walls of ovarian blood vessels. (*C*) Amyloid deposition in older area of hemorrhage (left). Note hemosiderin-laden macrophages (right).

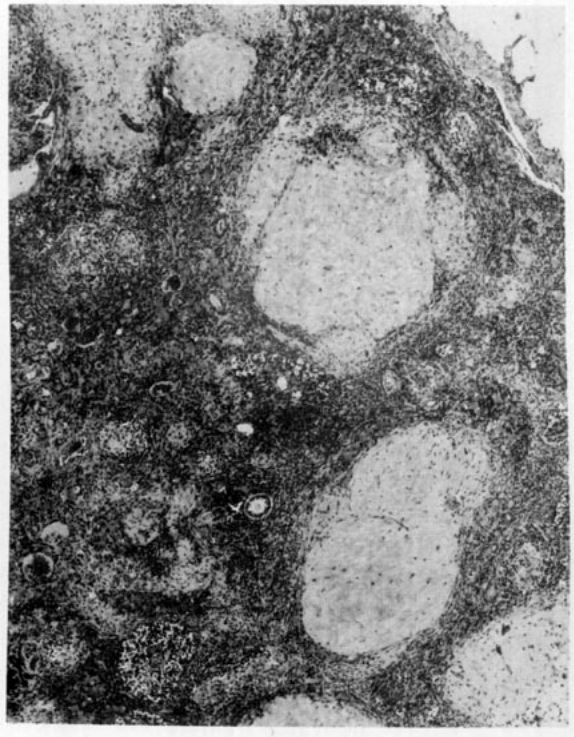

PLATE 10. Hyalin degeneration of corpora lutea in ovary of aged F344 rat.

PLATE 11. Low power photomicrograph of degenerative changes in corpora lutea of F344 rat ovary. (◀) Foci of thrombosis.

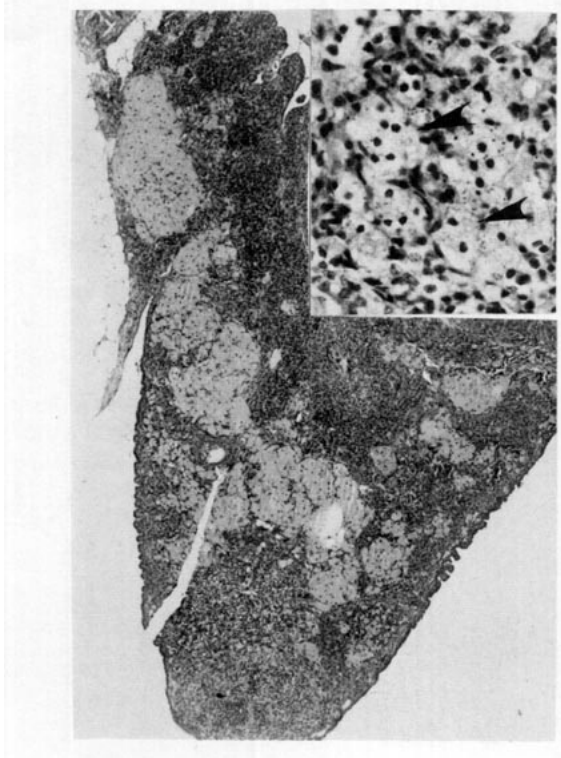

PLATE 12. Lipochrome (ceroid) pigment in ovary of F344 rat. Lightly stained areas are interstitial cells containing lipochrome pigment. Higher magnification (inset) shows intracytoplasmic pigment (◀) within ovarian interstitial cells.

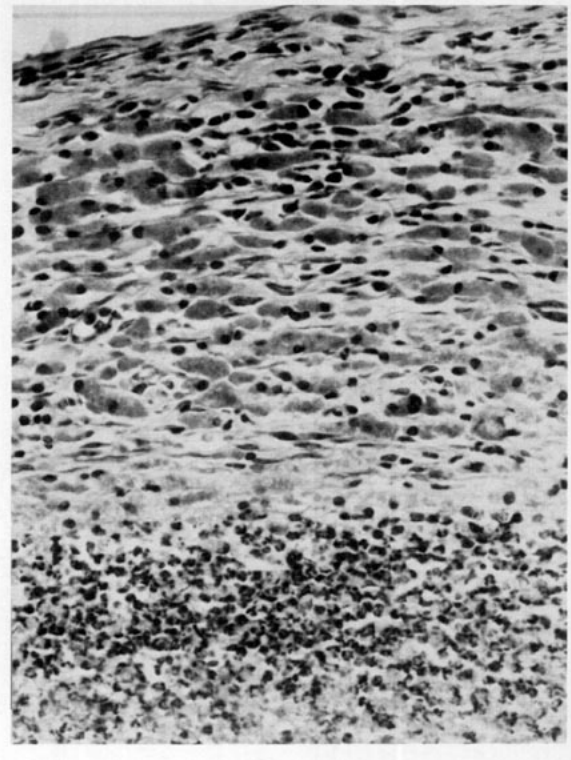

PLATE 13. Hemosiderin-laden macrophages in ovarian wall at site of chronic necrohemorrhagic inflammation in a B6C3F1 mouse.

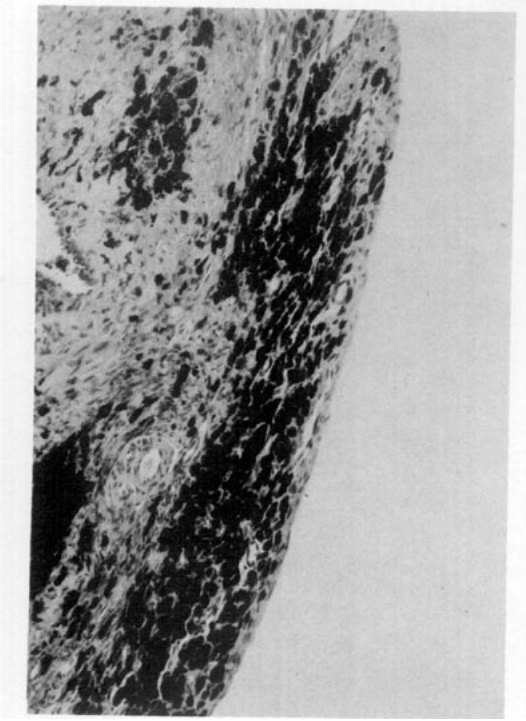

PLATE 14. Melanin pigment in the wall of an ovarian embryonic cyst in a B6C3F1 mouse.

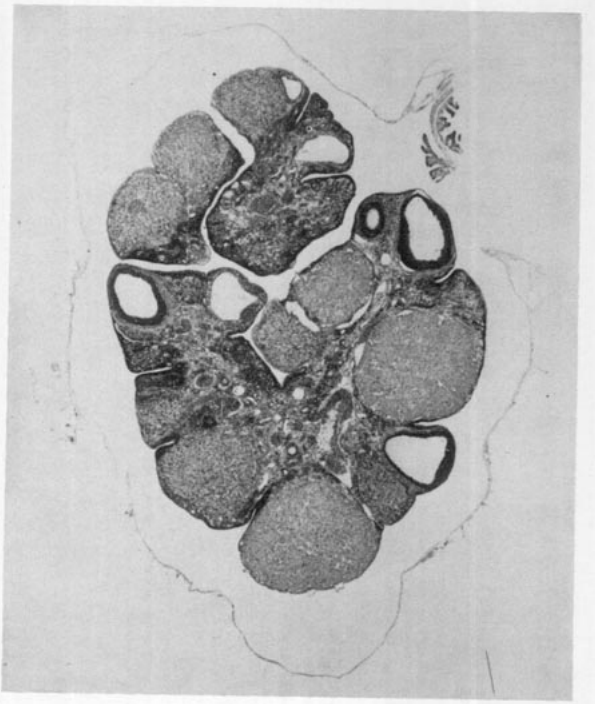

PLATE 15. Multiple, early, follicular cysts in a F344 rat. Note absence of oocytes and distention of the bursa.

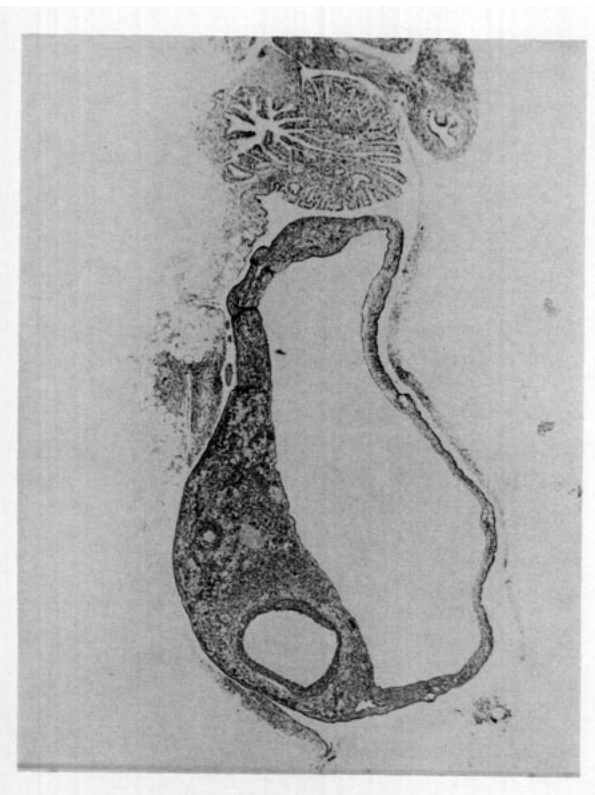

PLATE 16. Solitary follicular cyst in the ovary of an aged F344 rat.

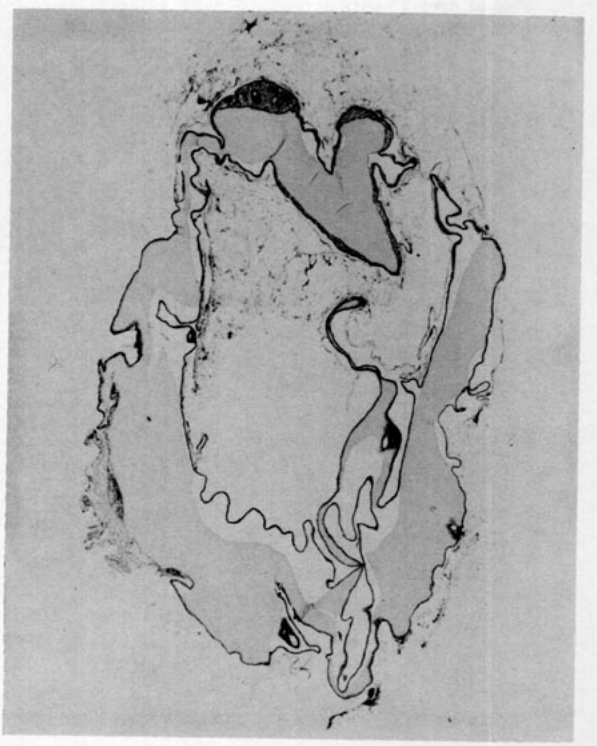

PLATE 17. Subgross photomicrograph of thin-walled polycystic ovary in aged F344 rat.

PLATE 18. Large follicular cyst containing hemorrhage and cholesterol clefts in a B6C3F1 mouse.

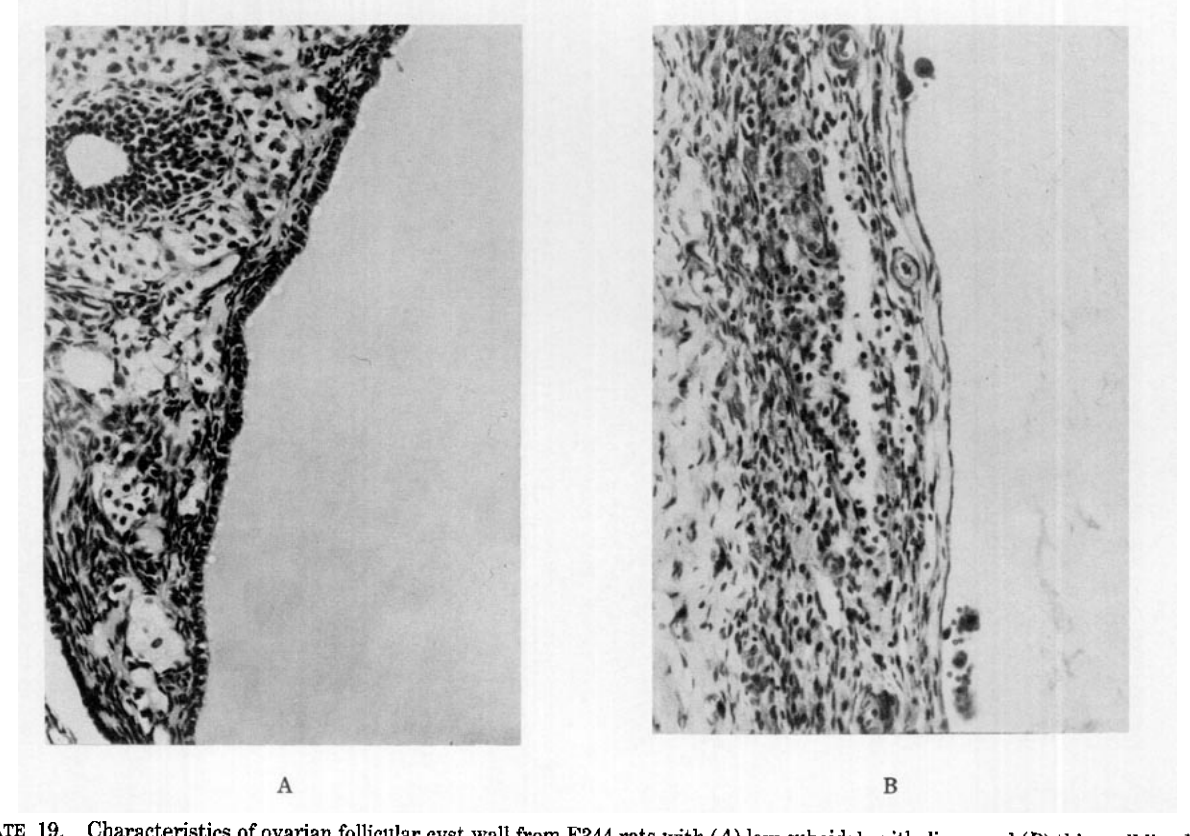

PLATE 19. Characteristics of ovarian follicular cyst wall from F344 rats with (*A*) low cuboidal epithelium; and (*B*) thin wall lined by squamous epithelium.

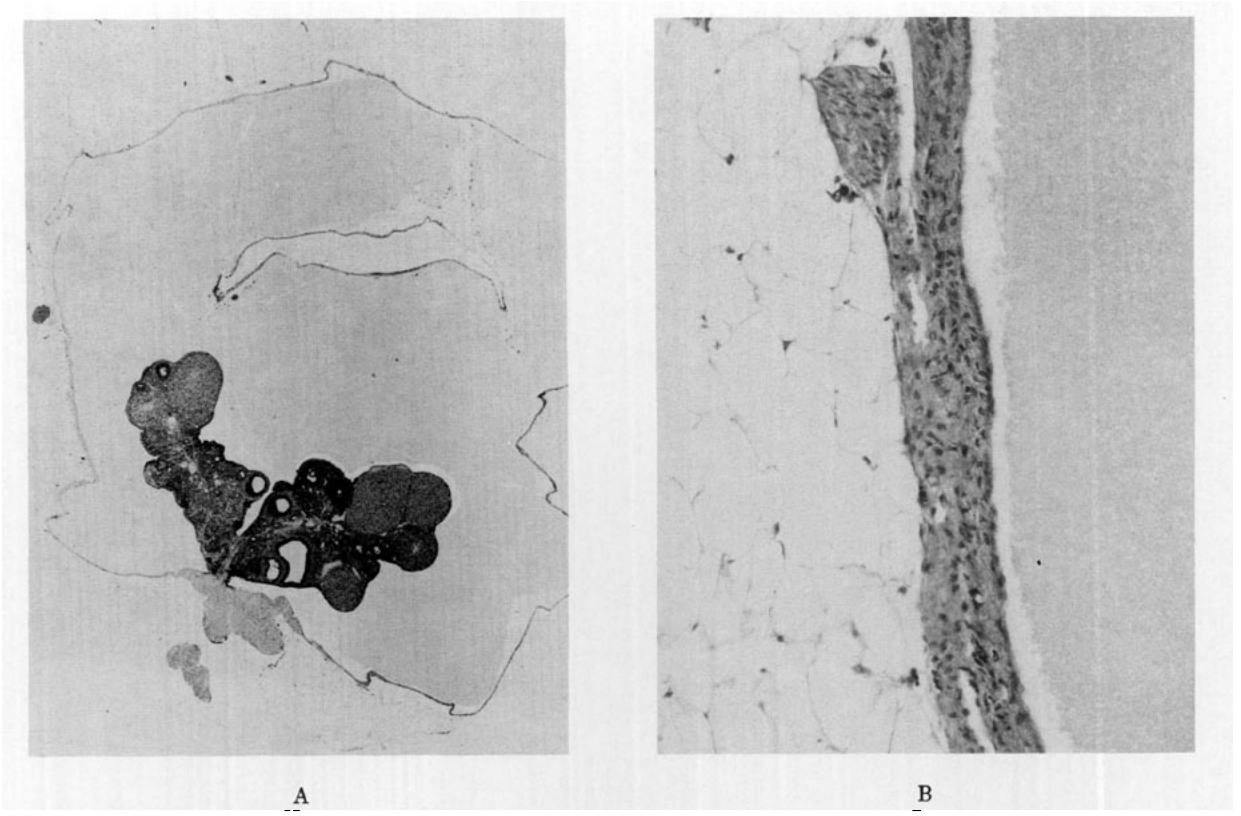

PLATE 20. Lutein cyst from a F344 rat. (*A*) Cyst contains proteinaceous fluid. (*B*) Cystic corpus luteum is lined by flattened epithelium. The wall contains several layers of granulosa cells with foamy cytoplasm containing a few fat vacuoles.

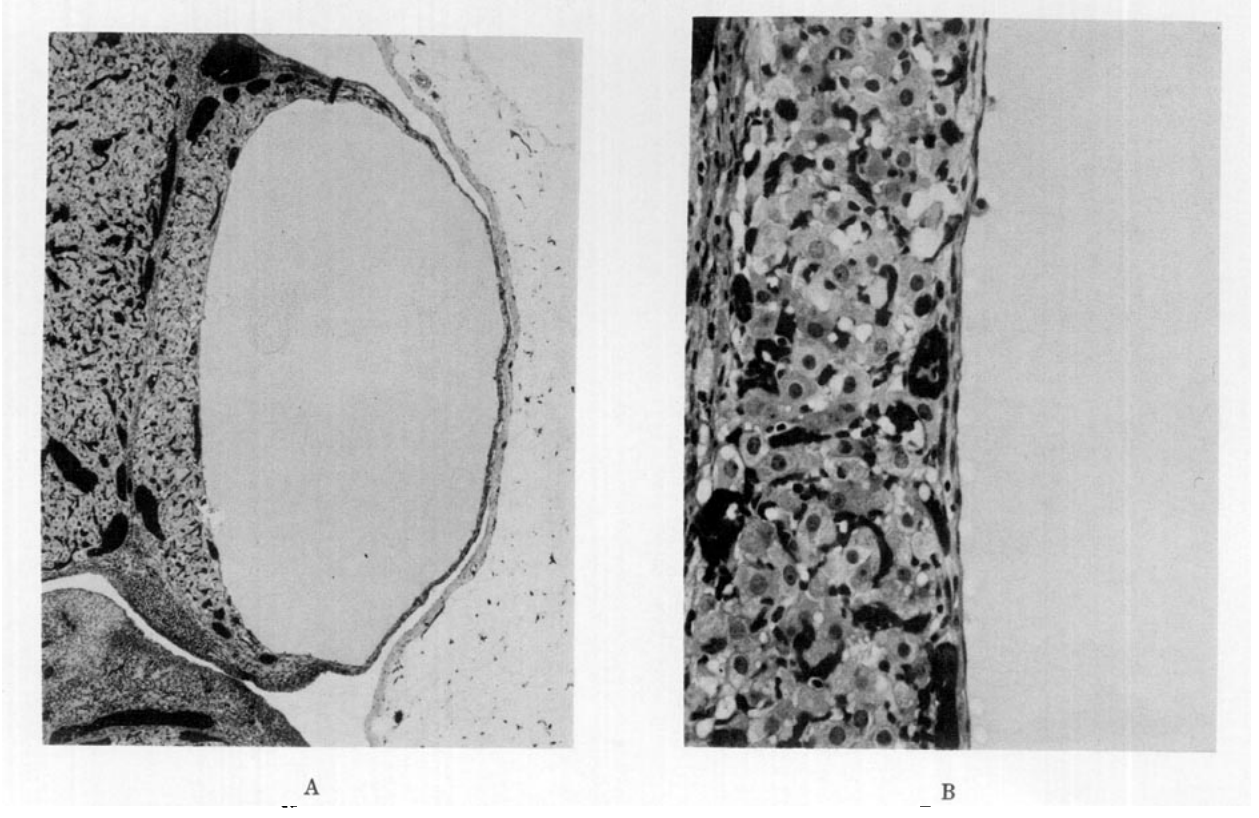

PLATE 21. (*A*) Large parovarian cyst from an aged F344 rat. (*B*) Smooth muscle in wall of cyst.

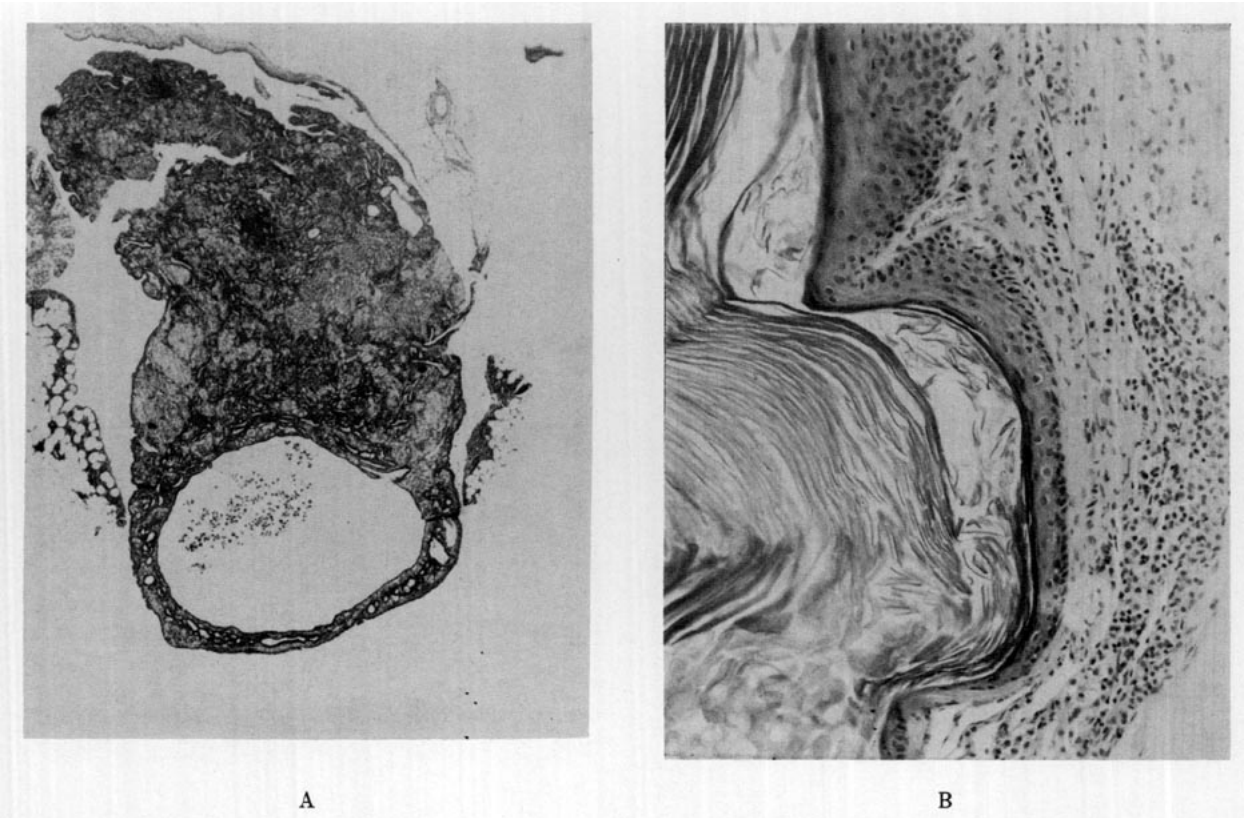

PLATE 22. Cystic rete tubule in ovary of B6C3F1 mouse. (*A*) Cystic distention of the rete tubule in one pole of the ovary. (*B*) Cystic rete. Note lack of smooth muscle in cyst wall.

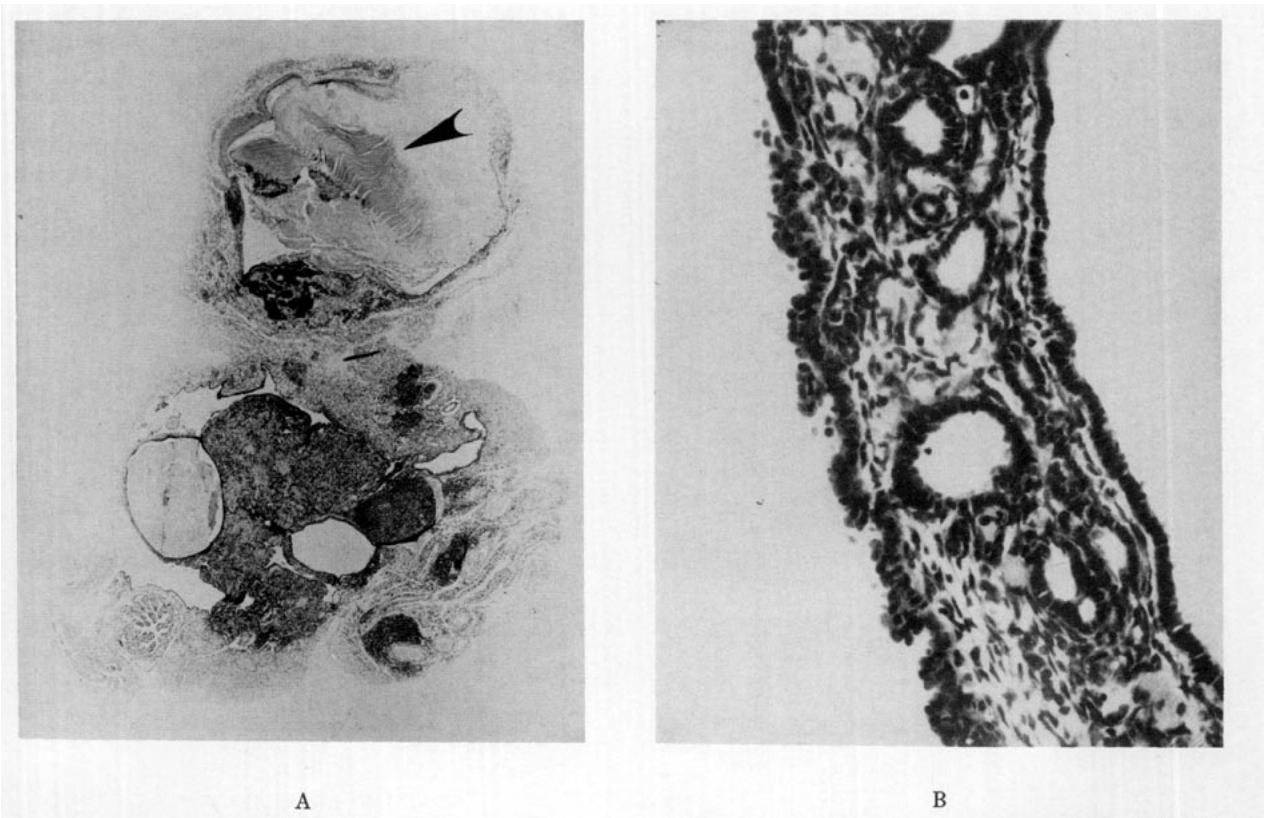

PLATE 23. Low power photomicrograph of an epidermoid cyst in a B6C3F1 mouse. (*A*) Note laminated appearance of keratin in cyst (◀). (*B*) Higher magnification shows stratified squamous epithelium in cyst wall with keratin production.

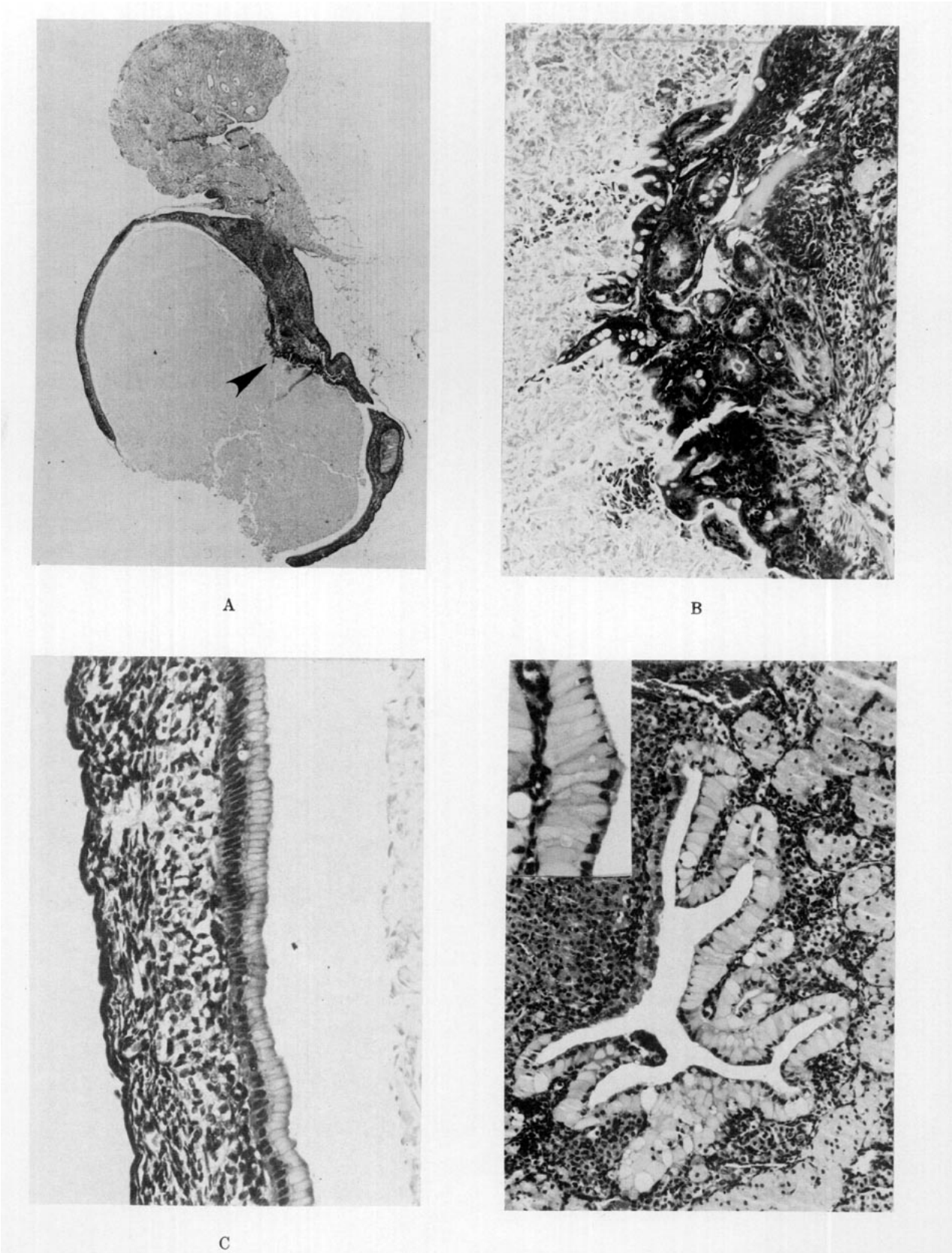

PLATE 24. Embryonic cyst in ovary of a B6C3F1 mouse. (*A*) Large cyst contains proteinaceous material. Note portion of cyst wall with papilliferous growth (▶). (*B*) Focal area within cyst wall contains glands and goblet cells similar to intestinal epithelium. (*C*) Balance of cyst wall contains high columnar epithelium with basilar nuclei and abundant eosinophilic cytoplasm.

PLATE 25. Ovarian embryonic cyst from a B6C3F1 mouse. Cyst has undulating border and is lined by pseudocolumnar epithelium with acidophilic globules and nuclei oriented toward the surface (inset).

A

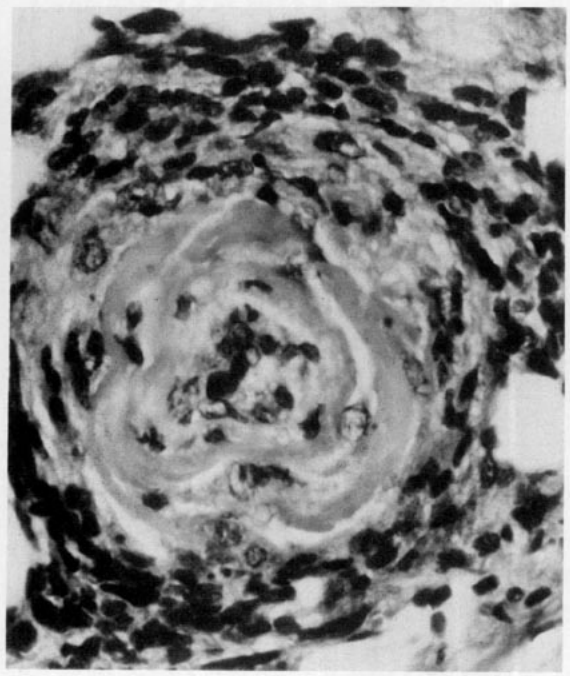

B

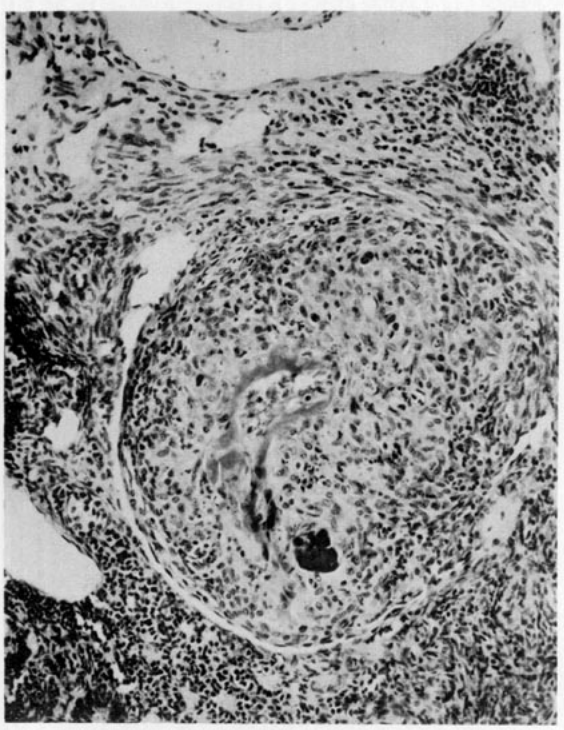

C

PLATE 26. Periarteritis of ovarian artery and its branches in B6C3F1 mice. (*A*) Medial hypertrophy. (*B*) Fibrinoid necrosis with perivascular inflammatory cell infiltration. (*C*) Necrotizing arteritis with thickening of the arterial wall, obliteration of the lumen, fibrinoid necrosis, and polymorphonuclear leukocytes in the media, and early periadventitial fibrosis.

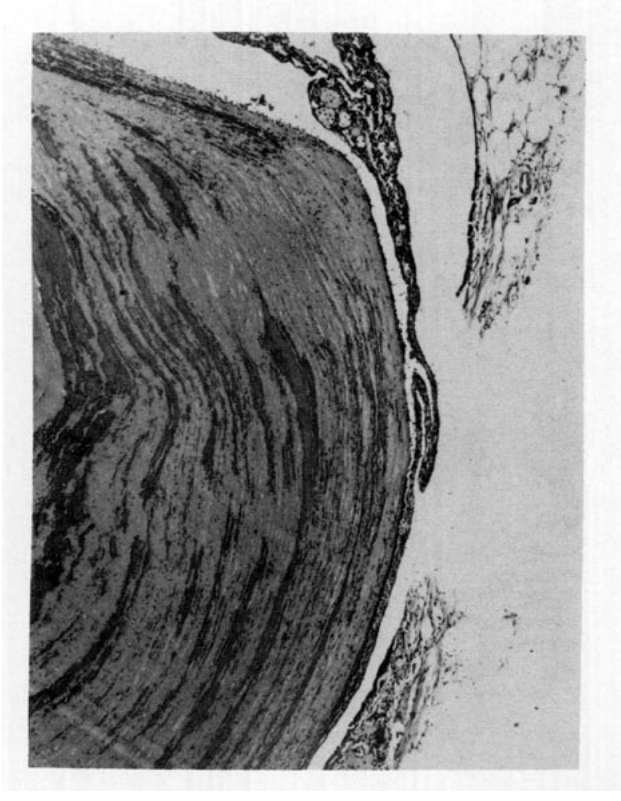

PLATE 27. Large hemorrhagic cyst in ovary of a B6C3F1 mouse. Lines of Zahn produce laminated appearance.

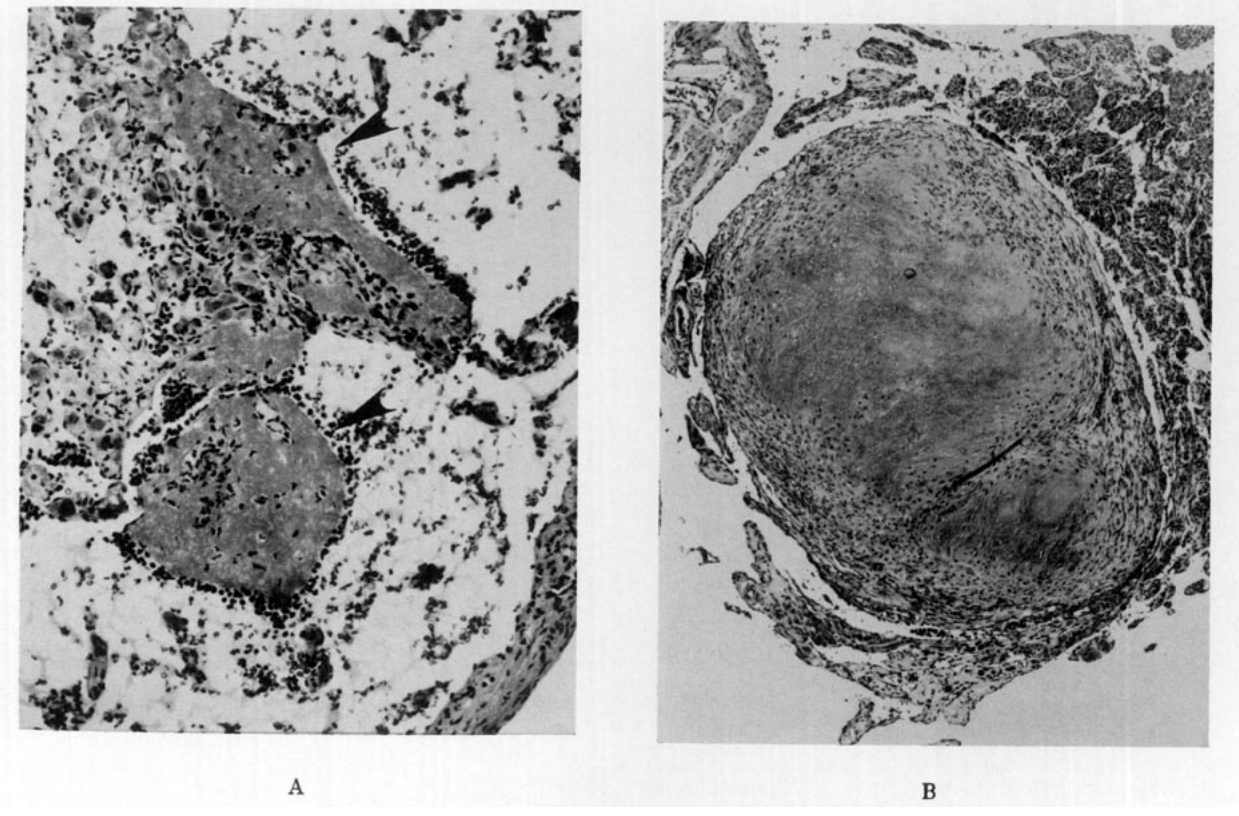

A B

PLATE 28. Ovarian thromboses. (*A*) Multiple thrombi (◀) in degenerating corpus luteum of a F344 rat. Note ring of polymorphonuclear leukocytes adherent to surface of thrombi. (*B*) Large organizing thrombus in ovarian artery of B6C3F1 mouse.

PLATE 29. Ovarian angiectasis in a B6C3F1 mouse. Photomicrograph demonstrates dilated vascular channels filled with blood and lined by endothelial cells.

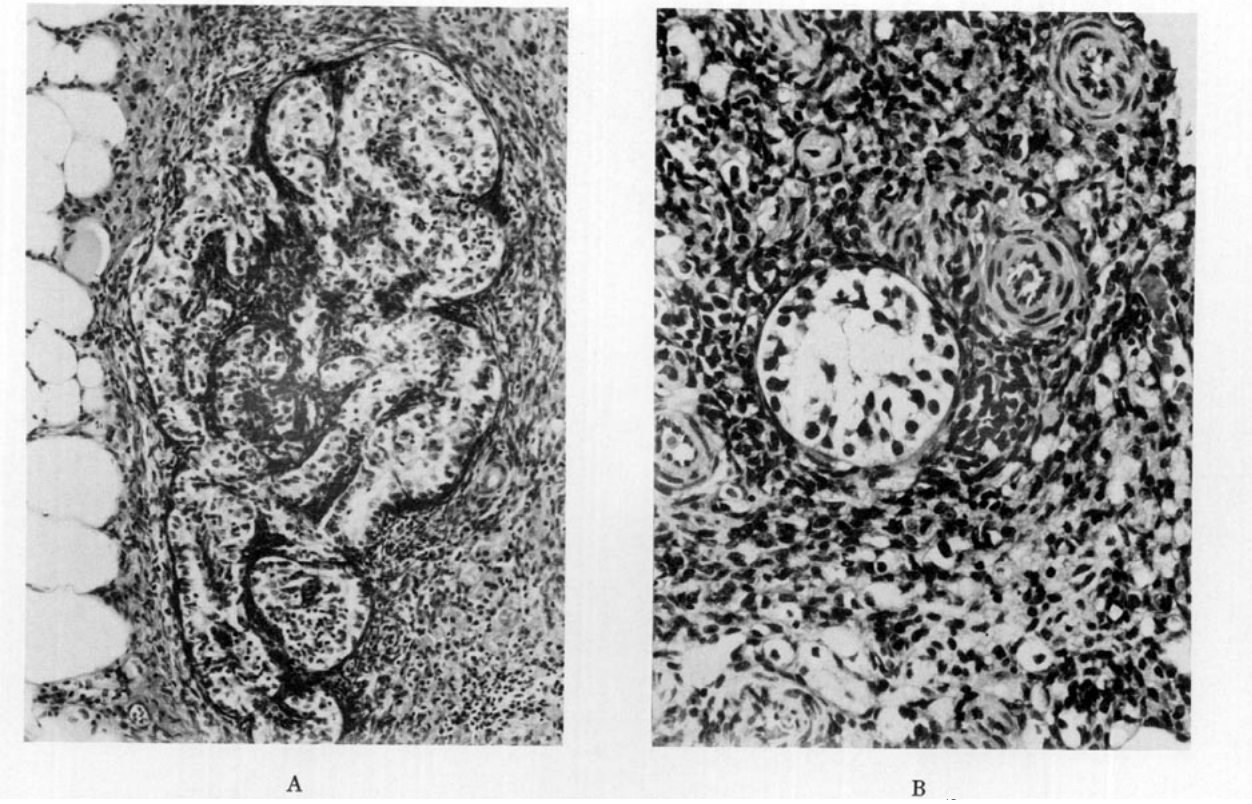

PLATE 30. Ovarian epithelial hyperplasia in the F344 rat. (*A*) Serpentine appearance of sertoli-like structures. Note distinct basement membrane and lack of spermatogenic elements. (*B*) Solitary Sertoli-like tubule in atrophic ovary.

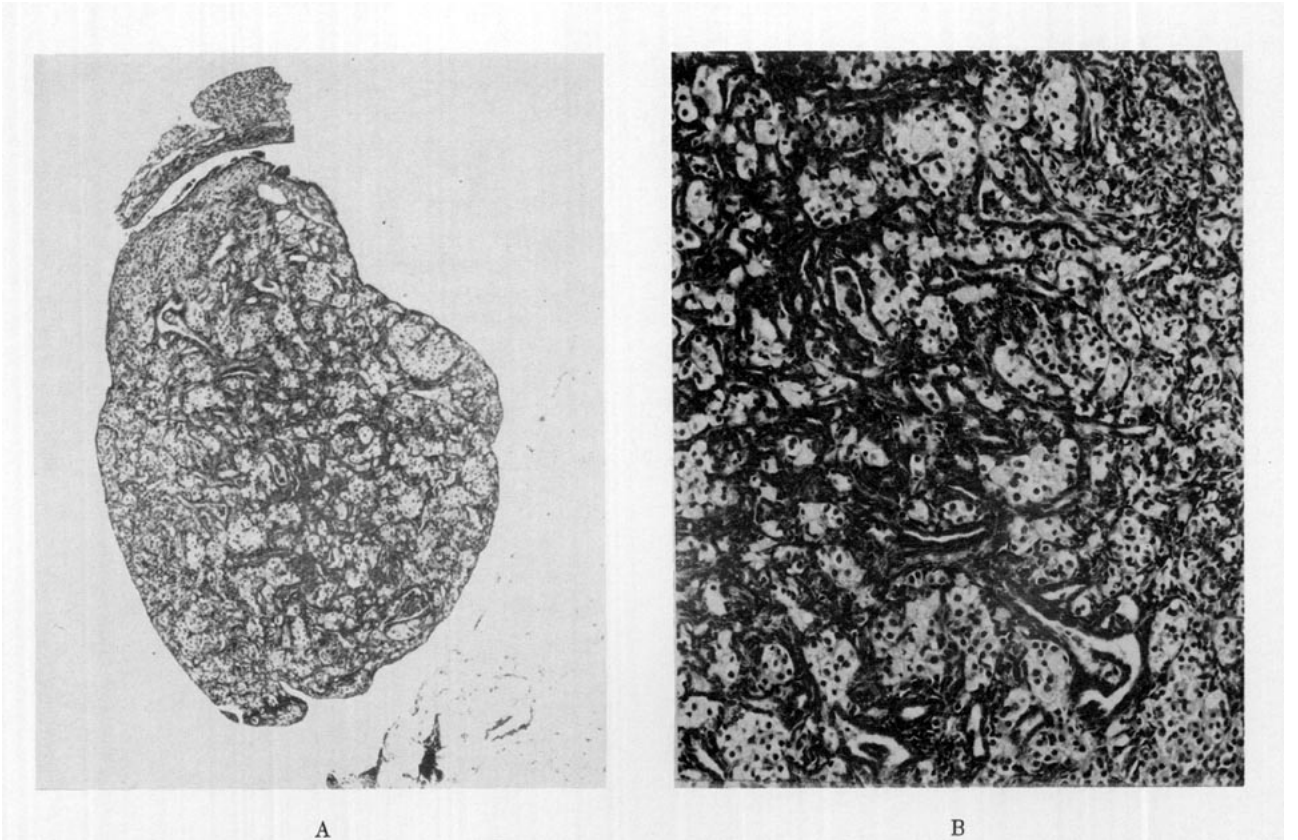

PLATE 31. Adenomatous hyperplasia of the ovary in B6C3F1 mice. (*A*) Low power photomicrograph demonstrating small ovary with downgrowth of the germinal epithelium. Note lack of follicles. (*B*) Higher magnification shows interstitial cells separated by interlacing clefts and tubules.

PLATE 32. Focal hyperplasia of interstitial cells in nonatrophic ovary of a F344 rat. Note packets of interstitial cells separated by delicate fibrovascular stroma (inset).

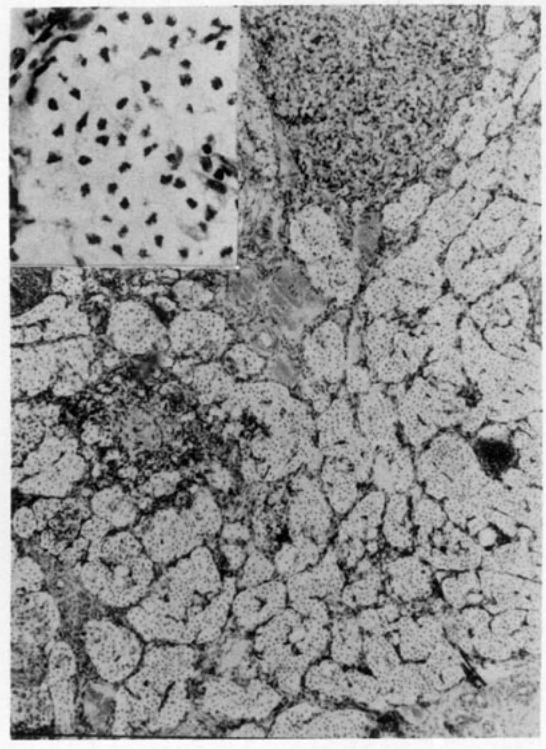

PLATE 33. Interstitial cell hypertrophy of the ovary in a F344 rat treated with tricresyl phosphate. Note replacement of ovary by islands of hypertrophied interstitial cells. Higher magnification (inset) demonstrating increased nuclear/cytoplasmic ratio. Note condensed nuclei and voluminous cytoplasm when compared to Plate 32.

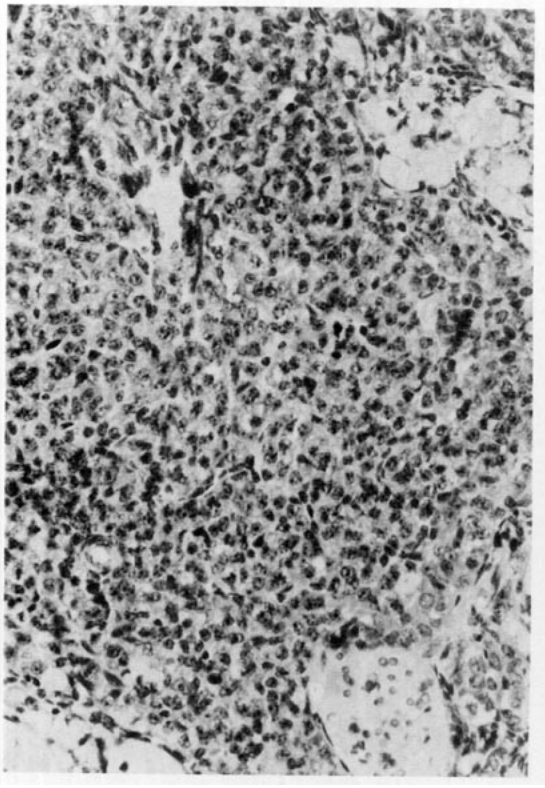

PLATE 34. Focal hyperplasia of granulosa cells in ovary of B6C3F1 mouse.

PLATE 35. Severe ovarian atrophy associated with aging in a B6C3F1 mouse. Reduced size can be compared to normal oviduct (▶).

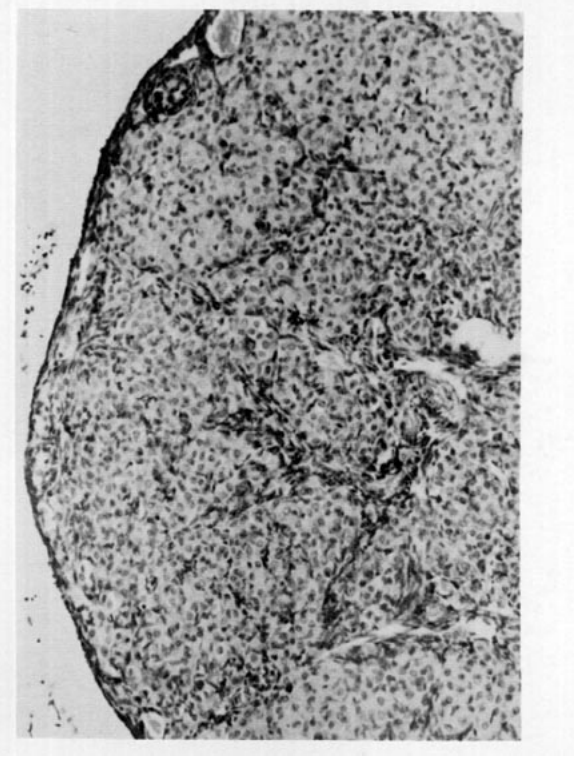

PLATE 36. Diffuse follicular atrophy in ovary of B6C3F1 mouse induced by treatment with vinylcyclohexene.